



**AFRL-SA-WP-TR-2018-0008**

# **Magnetic Resonance Imaging Following Single Exposure to Hypobarica and/or Hypoxia**



**Paul M. Sherman and John H. Sladky**

**April 2018**

**Final Report  
for May 2014 to August 2017**



**DISTRIBUTION STATEMENT A. Approved  
for public release. Distribution is unlimited.**

**Air Force Research Laboratory  
711<sup>th</sup> Human Performance Wing  
U.S. Air Force School of Aerospace Medicine  
Aeromedical Research Department  
2510 Fifth St., Bldg. 840  
Wright-Patterson AFB, OH 45433-7913**

# NOTICE AND SIGNATURE PAGE

Using Government drawings, specifications, or other data included in this document for any purpose other than Government procurement does not in any way obligate the U.S. Government. The fact that the Government formulated or supplied the drawings, specifications, or other data does not license the holder or any other person or corporation or convey any rights or permission to manufacture, use, or sell any patented invention that may relate to them.

Qualified requestors may obtain copies of this report from the Defense Technical Information Center (DTIC) (<http://www.dtic.mil>).

AFRL-SA-WP-TR-2018-0008 HAS BEEN REVIEWED AND IS APPROVED FOR PUBLICATION IN ACCORDANCE WITH ASSIGNED DISTRIBUTION STATEMENT.

//SIGNATURE//

---

DR. JAMES McEACHEN  
CRCL, Human Performance

//SIGNATURE//

---

DR. RICHARD A. HERSACK  
Chair, Aeromedical Research Department

This report is published in the interest of scientific and technical information exchange, and its publication does not constitute the Government's approval or disapproval of its ideas or findings.

| <b>REPORT DOCUMENTATION PAGE</b>  |                         |   | <i>Form Approved</i><br><i>OMB No. 0704-0188</i>                               |   |  |
|---|-------------------------|---|--|---|--|
| Public reporting burden for this collection of information is estimated to average 1 hour per response, including the time for reviewing instructions, searching existing data sources, gathering and maintaining the data needed, and completing and reviewing this collection of information. Send comments regarding this burden estimate or any other aspect of this collection of information, including suggestions for reducing this burden to Department of Defense, Washington Headquarters Services, Directorate for Information Operations and Reports (0704-0188), 1215 Jefferson Davis Highway, Suite 1204, Arlington, VA 22202-4302. Respondents should be aware that notwithstanding any other provision of law, no person shall be subject to any penalty for failing to comply with a collection of information if it does not display a currently valid OMB control number. <b>PLEASE DO NOT RETURN YOUR FORM TO THE ABOVE ADDRESS.</b>   |                         |   |  |   |  |
| <b>1. REPORT DATE (DD-MM-YYYY)</b><br>23 Apr 2018   |                         | <b>2. REPORT TYPE</b><br>Final Technical Report |  | <b>3. DATES COVERED (From – To)</b><br>May 2014 – August 2017 |  |
| <b>4. TITLE AND SUBTITLE</b><br><br>Magnetic Resonance Imaging Following Single Exposure to Hypobaria and/or Hypoxia  |                         |   | <b>5a. CONTRACT NUMBER</b>   |   |  |
|   |                         |   | <b>5b. GRANT NUMBER</b>  |   |  |
|   |                         |   | <b>5c. PROGRAM ELEMENT NUMBER</b>  |   |  |
| <b>6. AUTHOR(S)</b><br><br>Paul M. Sherman, John H. Sladky  |                         |   | <b>5d. PROJECT NUMBER</b><br>14-004  |   |  |
|   |                         |   | <b>5e. TASK NUMBER</b>   |   |  |
|   |                         |   | <b>5f. WORK UNIT NUMBER</b>  |   |  |
| <b>7. PERFORMING ORGANIZATION NAME(S) AND ADDRESS(ES)</b><br>USAF School of Aerospace Medicine<br>Aeromedical Research Dept/FHOH<br>2510 Fifth St., Bldg. 840<br>Wright-Patterson AFB, OH 45433-7913  |                         |   | <b>8. PERFORMING ORGANIZATION REPORT NUMBER</b><br><br>AFRL-SA-WP-TR-2018-0008 |   |  |
| <b>9. SPONSORING / MONITORING AGENCY NAME(S) AND ADDRESS(ES)</b>  |                         |   | <b>10. SPONSORING/MONITOR'S ACRONYM(S)</b>                                     |   |  |
|   |                         |   | <b>11. SPONSOR/MONITOR'S REPORT NUMBER(S)</b>                                  |   |  |
| <b>12. DISTRIBUTION / AVAILABILITY STATEMENT</b><br><br>DISTRIBUTION STATEMENT A. Approved for public release. Distribution is unlimited.   |                         |   |  |   |  |
| <b>13. SUPPLEMENTARY NOTES</b><br>Cleared, AFIMSC/PA, Case # 2018-0182, 29 May 2018.  |                         |   |  |   |  |
| <b>14. ABSTRACT</b><br>Subcortical white matter (WM) injury and global decreased fractional anisotropy are associated with repetitive exposure to nonhypoxic hypobaric conditions, in both aerospace physiology inside observers and high-altitude U-2 pilots. A single hypobaric hypoxic occupational exposure to 7620 meters (5.45 psi) induces magnetic resonance imaging (MRI) changes that reflect transient brain injury. Ninety-six U.S. Air Force aircrew trainees and 14 aerospace physiology inside observers undergoing occupational altitude chamber training exposure to 7620 meters (5.45 psi) and 65 age-matched control subjects were evaluated. Subjects underwent MRI brain examinations (Siemens 3T Verio magnet) 24 hours pre-exposure and 24 and 72 hours post-exposure with quantification of findings. MRI protocol included fluid-attenuated inversion recovery images, magnetic resonance spectroscopy within the frontal WM and anterior cingulate gyrus, diffusion-weighted imaging, and arterial spin labeling perfusion imaging. Statistical analysis was performed with a generalized additive model and paired two-tailed t-tests. Arterial spin labeling showed an upregulation of white and gray matter cerebral blood flow (CBF) at both 24 and 72 hours in the exposed subjects (WM $p = 0.003/0.020$ ; gray matter $p = 0.053/0.041$ ). Group comparison using a generalized additive model adjusted for age and gender demonstrated significant increased WM CBF at 24 and 72 hours post-exposure compared to controls ( $p < 0.001$ and $p = 0.048$ , respectively). There is no statistical difference in CBF between the 24- and 72-hour MRIs. No significant change in CBF was observed in the control subjects. There were no WM fluid-attenuated inversion recovery changes. Results demonstrate an upregulation of WM CBF following exposure to occupational hypobaric training that persists up to 72 hours following exposure. Data reflect an increased metabolic demand and suggest a transient cerebral injury has occurred. Repetitive injury with repetitive hypobaric exposure, without adequate time for healing, may represent an underlying basis for previously reported subcortical WM injury. |                         |   |  |   |  |
| <b>15. SUBJECT TERMS</b><br>White matter hyperintensities, high-altitude, hypobaria, hypoxia, magnetic resonance imaging  |                         |   |  |   |  |
| <b>16. SECURITY CLASSIFICATION OF:</b>  |                         |   | <b>17. LIMITATION OF ABSTRACT</b>  | <b>18. NUMBER OF PAGES</b>                                    | <b>19a. NAME OF RESPONSIBLE PERSON</b><br>Dr. Paul Sherman |
| <b>a. REPORT</b><br>U   | <b>b. ABSTRACT</b><br>U | <b>c. THIS PAGE</b><br>U                        |  |   | <b>19b. TELEPHONE NUMBER (include area code)</b>           |
|   |                         |   | SAR  | 26  |  |

*This page intentionally left blank.*

# TABLE OF CONTENTS

|   | <b>Page</b> |
|---|-------------|
| LIST OF FIGURES .....   | ii          |
| LIST OF TABLES .....  | ii          |
| 1.0 SUMMARY .....   | 1           |
| 2.0 INTRODUCTION .....  | 1           |
| 3.0 RISK ANALYSIS.....  | 2           |
| 4.0 METHODS .....   | 2           |
| 4.1 Participants.....   | 2           |
| 4.2 Hypobaric and Hypoxic Exposure Procedures .....                                     | 3           |
| 4.3 MRI Procedure.....  | 4           |
| 4.4 Statistical Analysis.....   | 7           |
| 5.0 RESULTS .....   | 7           |
| 5.1 Overall Limitations/Challenges .....  | 7           |
| 5.2 Reproducibility of Quantitative Structural and Physiological MRI Measurements ..... | 7           |
| 5.3 Multimodal WM Responses to Hypoxic Hypobaria in Humans .....                        | 16          |
| 6.0 DISCUSSION .....  | 17          |
| 7.0 CONCLUSIONS.....  | 18          |
| 8.0 REFERENCES .....  | 18          |
| LIST OF ABBREVIATIONS AND ACRONYMS .....  | 19          |

## LIST OF FIGURES

|  | <b>Page</b> |
|--|-------------|
| Figure 1. Initial chamber flight profile .....               | 3           |
| Figure 2. Rapid decompression hypobaric chamber flight ..... | 3           |

## LIST OF TABLES

|   | <b>Page</b> |
|---|-------------|
| Table 1. Consistency of FLAIR .....   | 8           |
| Table 2. Consistency of Cortical Thickness .....  | 8           |
| Table 3. Consistency of FA Derived from DTI .....   | 11          |
| Table 4. Consistency of MBI (or q-space) for Corpus Callosum and Anterior Cingulate ..... | 11          |
| Table 5. Consistency of GM Blood Flow as Measured by pCASL.....                           | 12          |
| Table 6. Consistency of WM Blood Flow as Measured by pCASL.....                           | 14          |
| Table 7. Consistency of Proton MRS .....  | 15          |
| Table 8. Arterial Spin Labeling Changes in White and Gray Matter .....                    | 17          |

## 1.0 SUMMARY

Occupational exposure to nonhypoxic hypobaric (low atmospheric pressure) conditions in aircrew is associated with focal and diffuse white matter (WM) injury with an associated acquired decrement in neurocognitive function. These magnetic resonance imaging changes may occur in the absence of decompression sickness symptoms. Similar focal WM change occurs in extreme mountaineers and in divers exposed to hypobaria. These pathological changes are likely triggered by transient occlusion from macro- or microarterial gas emboli or neutrophil activation with microembolic or microparticle damage, potentially with activation of innate immune responses. The extent of the WM injury may not correlate with cumulative exposure hours, suggesting that other factors such as the level of physical and mental activity during exposure, exposure frequency and time between exposures, and/or other environmental and genetic susceptibility risks may be relevant.

We demonstrated highly reproducible magnetic resonance imaging data for neuroimaging measurements, making them valuable for evaluation of disease states and treatment protocols. We demonstrated compelling evidence of transient brain injury from a single exposure to hypobaria as evidenced by increased CBF, persisting at 72 hours post-exposure, and transient neurometabolite changes (glutathione, choline, glutamate, N-acetylaspartate, myo-inositol, creatine). The duration of elevated CBF after a single altitude chamber hypobaric exposure is not yet known. Changes in CBF may be driven by neurometabolite changes. A higher WM hyperintensity baseline burden seems to predict greater CBF change (significant in WM arterial spin labeling data). This suggests a potential underlying susceptibility to injury. There is also a potential synergetic interaction between hypobaric exposure and hypoxia. WM hyperintensities in pilots/aircrew are likely a function of both frequency and cumulative effects of decompressive stress from hypobaric exposure.

## 2.0 INTRODUCTION

Since 2006, repeated episodes of neurological decompression sickness have been observed in the U.S. Air Force (USAF) high-altitude U-2 population [1]. Increased volume and count of subcortical white matter hyperintensities (WMH) have been measured in high-altitude U-2 pilots and in altitude chamber physiology personnel [2-4]. These changes have been associated with acquired cognitive change on neurocognitive testing consistent with subcortical injury [5]. The pathophysiology behind these changes remains unclear. We previously hypothesized that acute exposure to hypobaria produces a showering of microemboli ( $\leq 30 \mu\text{m}$ ) that impact the deep cerebral white matter (WM), initially inciting a change in small arteriole vascular integrity with alteration in diffusion coefficient on magnetic resonance imaging (MRI) followed by subsequent WMH change on fluid-attenuated inversion recovery (FLAIR) MRI. Cognitive change on MicroCog neurocognitive testing would follow this injury. The nature of these microemboli remains unclear – possibilities include microbubbles, “macro” microparticles with a gaseous phase, fibrin/platelet aggregates, or other unknown microemboli. We currently believe these microemboli may contribute to a local inflammatory reaction, possibly contributing to the MRI and microcognitive changes. Additionally, if the brain injury is secondary to disruption of vascular integrity and/or inflammatory changes occurring at the vascular endothelial level, then we would anticipate similar changes might occur following hypoxic exposure [6]. Still missing is evidence of degree of acute injury and temporal resolution in

humans following a single exposure to hypobaria and/or hypoxia. Assessment of the degree of injury and/or change and temporal resolution occurring in association with exposure to hypobaria and/or hypoxia will permit operational adjustments that will optimize mission needs while mitigating subcortical WM injury in aircrew.

This study examined subjects already participating in occupational hypobaric and/or hypoxic exposure as part of routine USAF aircrew qualification/requalification. We hypothesized a single exposure such as occurs during routine aircrew training will induce transient change in cerebral deep WM water movement that can be demonstrated on multiphase diffusion tensor imaging (DTI). By examining the arterial spin labeling (ASL), we determined the relative contribution of vascular change versus intracellular/extracellular water change. Additionally, by examining magnetic resonance spectroscopy (MRS) data, we hypothesized a single exposure would induce changes in cerebral metabolites, which might correlate with serological data analysis acquired at the same time. By performing serial imaging on subjects, we demonstrated the temporal resolution course.

### **3.0 RISK ANALYSIS**

The study involved minimal risk because MRI uses low-energy, non-ionizing radio waves, there were no known risks or side effects, and there were no reported issues for the duration of the study. There was a possibility of discovering a medically disqualifying condition in the volunteer subjects, but this did not occur.

## **4.0 METHODS**

### **4.1 Participants**

The study was reviewed and approved by the Air Force Research Laboratory Institutional Review Board. All pilot and control subjects were active duty members of the U.S. Armed Forces. Calibration (CAL) subjects, recruited to permit cross-comparison of the two scanners utilized in this study, were active duty or retired military beneficiaries. All participants were recruited with strict adherence to the Department of Defense Instruction for Protection of Human Subjects. For all subjects, participation was voluntary without commander involvement or knowledge. All subjects provided informed consent prior to participation. Subjects did not receive compensation for participation. A total of 186 subjects underwent testing, completed as of 14 September 2017, which included 96 Aircrew Fundamentals Course volunteers, 14 aerospace physiology crew members, 3 qualified candidates for refresher training with the reduced oxygen breathing device, and 73 normal controls.

## 4.2 Hypobaric and Hypoxic Exposure Procedures

The objective of standard USAF hypobaric altitude chamber training is for early aircrew recognition of hypoxic symptoms while still retaining sufficient cognitive ability to respond [7]. Standard protocol includes a brief ear and sinus check exposure at 5000 feet (exposure 12.2 psi/632 mmHg/ambient air oxygen (O<sub>2</sub>) via aviator mask >500 mmHg) followed by 30 minutes of denitrogenation on 100% O<sub>2</sub> at sea level via an aviator mask. Trainees then ascend to 25,000 feet (exposure 5.45 psi/282 mmHg/ambient air O<sub>2</sub> via aviator mask >200 mmHg) where they remain for 20 minutes. Trainees remove their aviator masks, redonning with the first onset of hypoxic symptoms. Total duration of mask removal at altitude is approximately 2-5 minutes with an O<sub>2</sub> saturation reaching 65-75% (exposure 5.45 psi/282 mmHg/ambient air O<sub>2</sub> 59 mmHg). Following recovery on 100% O<sub>2</sub> via aviator mask, trainees descend to 18,000 feet for a visual acuity demonstration followed by continued descent to sea level (Figures 1 and 2). This training procedure is standard for all USAF aircrew recruits. Although decompression sickness (DCS) rarely does occur with this protocol, no subjects in this study experienced DCS symptoms.

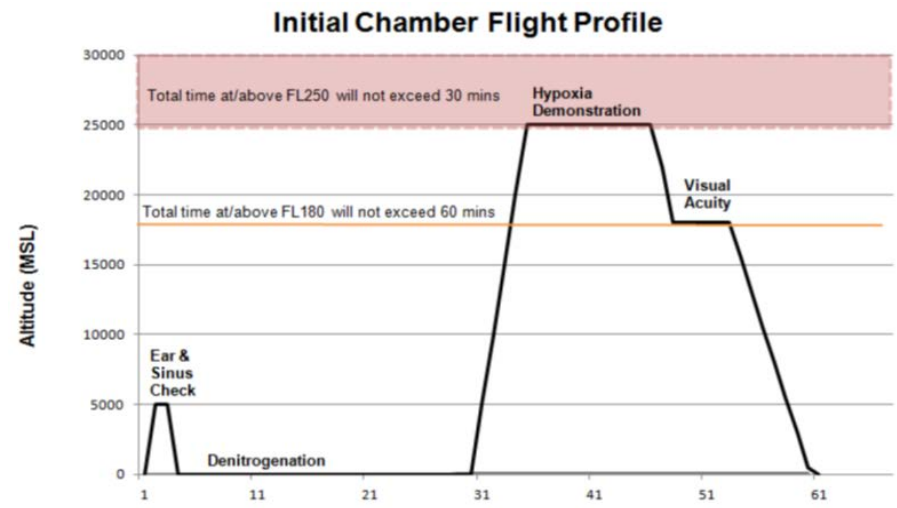


Figure 1. Initial chamber flight profile. From Air Force Instruction 11-403 [7].

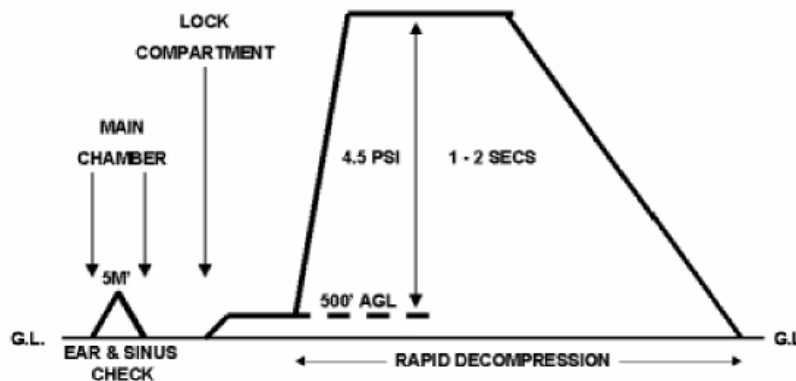


Figure 2. Rapid decompression hypobaric chamber flight. From Air Force Instruction 11-403 [7].

The reduced oxygen breathing device (ROBD) uses a mixed gas solution delivered via aviator mask. Thermal mass flow controllers mix breathing air and nitrogen to produce the sea level equivalent atmospheric oxygen contents for altitudes up to 34,000 feet. The mass flow controllers are calibrated on a primary flow standard traceable to the National Institute of Standards and Technology.

### 4.3 MRI Procedure

Imaging data were collected at the Wilford Hall Ambulatory Surgical Center (WHASC), 59<sup>th</sup> Medical Wing, Joint Base San Antonio – Lackland, TX, using a Siemens 3T Verio scanner equipped with a 32-channel phase array coil. Calibration imaging data were previously obtained at both the Research Imaging Institute and WHASC. Both scanners are operated under quality control and assurance guidelines in accordance with recommendations by the American College of Radiology. Three-dimensional FLAIR was utilized for WMH analysis. FLAIR images were coregistered to a common Talairach atlas-based stereotactic frame. An experienced neuroanatomist blinded to group manually traced WMH while a neuroradiologist blinded to clinical history provided MRI interpretation. For each lobe we manually counted the number of WMH (count) and used in-house software to compute the total volume of WMH (volume). WMH were divided into periventricular (adjacent to the ventricles) and subcortical; we considered only the subcortical WMH burden to be significant, since only the subcortical WMH burden correlates with hypobaric stress. Three-dimensional imaging parameters were T1 MPRAGE: repetition time (TR) = 2200 ms, echo time (TE) = 2.85 ms, isotropic resolution 0.80 mm, and FLAIR: TR = 4500 ms, TE = 1 ms, and isotropic resolution 1.00 mm.

High angular resolution diffusion imaging (HARDI) was utilized for DTI and fractional anisotropy (FA) data. Briefly, DTI data were collected using a single-shot echo-planar, single refocusing spin-echo, T2-weighted sequence with a spatial resolution of  $1.7 \times 1.7 \times 3.0$  mm with sequence parameters of TE/TR = 87/8000 ms, field of view (FOV) = 200 mm, axial slice orientation with 50 slices and no gaps, 64 isotropically distributed diffusion-weighted directions, two diffusion weighting values ( $b = 0$  and  $700 \text{ s} \cdot \text{mm}^{-2}$ ), and five  $b = 0$  images. HARDI data for both groups were processed using the freely available ENIGMA (enhanced neuro imaging genetics by meta-analysis)-DTI pipeline (<http://enigma.ini.usc.edu/protocols/dti-protocols/>), which consists of a set of protocols and scripts to measure average whole-brain FA value and average tract FA values for 10 major WM tracts [corpus callosum (CC), corticospinal (CS), internal capsule (IC), corona radiata (CR), thalamic radiation (Tr), sagittal stratum (SS), external capsule (EC), cingulum (Cing), superior longitudinal fasciculus (SLF), and fronto-occipital (FO)]. We chose the ENIGMA-DTI analysis protocol because it can effectively overcome the impact of the punctate WMH lesions on FA values compared to simple averaging of FA values within a region of interest, effectively limiting analysis of FA values to that of the normal-appearing WM.

We selected three commonly used statistical metrics to provide a thorough assessment of reproducibility of MRI/MRS performed over a short interval in normal healthy volunteers. These metrics serve as the foundation for statistical inferences of the effects of disease or treatment on brain structure and/or physiology over time as measured by MRI/MRS. We used the variance observed across the three visits to perform a power analysis to calculate a hypothetical group size that is necessary to detect 3% and 10% group differences using a two-tailed t-test. This information should help to perform power analyses for the neuroimaging studies that utilize these measurements.

The diffusion-weighted imaging protocol consisted of 15 shells of  $b$ -values ( $b = 250, 500, 600, 700, 800, 900, 1000, 1250, 1500, 1750, 2000, 2500, 3000, 3500, \text{ and } 3800 \text{ s/mm}^2$ ; diffusion gradient duration = 47 ms, diffusion gradient separation = 54 ms). Thirty isotropically distributed diffusion-weighted directions were collected per shell, including 16  $b = 0$  images. The highest  $b$ -value ( $b = 3800 \text{ s/mm}^2$ ) was chosen because the signal-to-noise ratio (SNR) for the CC in the average diffusion image (SNR =  $6.1 \pm 0.7$ ) measured in five healthy volunteers (ages 25-50 years) during protocol development approached the empirically selected lower limit of SNR = 5.0. The  $b$ -values and the number of directions per shell were chosen for improved fit of the bi-exponential model and SNR. The imaging data were collected using a single-shot, echo-planar, single refocusing spin-echo, T2-weighted sequence with a spatial resolution of  $1.7 \times 1.7 \times 4.6 \text{ mm}$  and seven slices prescribed in sagittal orientation to sample the midsagittal band of the CC. The sequence control parameters were TE/TR = 120/1500 ms with the FOV = 200 mm. The total scan time was about 10 minutes per subject. The permeability-diffusivity model addresses a limitation of the standard DTI-FA model, which assumes a single pool of anisotropically diffusing water. However, diffusion signal behaves as a bi-exponential function of  $b$ -values, representing two, unrestricted and restricted, “pools” of water ( $M_u$  and  $M_r$ , respectively). Parameters derived from the bi-exponential modeling, such as the permeability-diffusivity index (PDI), are therefore sensitive to membrane permeability. In short, diffusion images were preprocessed to perform a region of interest based fit for a two-compartment diffusion model (Equation 1) that assumed that intravoxel signal is formed by a contribution from two compartments.

$$S(b) = S_0 \cdot [M_u \cdot e^{-bD_u} + M_r(1 - M_u) \cdot e^{-bD_r}] \quad (1)$$

where  $S(b)$  is the average diffusion-weighted signal for a given  $b$ -value, averaged across all directions,  $M_u$  is the fraction of the signal that comes from the compartment with unrestricted diffusion, and  $M_r(1 - M_u)$  is the fraction of the signal that comes from the compartment with restricted diffusion.

The PDI was calculated as the ratio of  $D_u$  and  $D_r$  (Equation 2), which are the apparent diffusion coefficients of the unrestricted and restricted compartments, respectively.

$$PDI = D_r/D_u \quad (2)$$

The diffusion-weighted image for each of the  $b$ -values,  $S(b)$ , was calculated for the four regions of interest in cerebral WM (the whole and the genu, body, and splenium of CC) and for the gray matter (GM) of the cingulate gyrus.

Pseudocontinuous ASL (pCASL; RRID:SCR\_015004) imaging data for GM and WM were collected using gradient-echo echo-planar imaging with TE/TR = 16/4000 ms, 24 contiguous slices with 5-mm slice thickness, matrix =  $64 \times 64$ ,  $3.44 \times 3.44 \times 5.00$  mm resolution (FOV = 220 mm) labeling gradient = 0.6 G/cm, bandwidth = 1594 Hz/pixel, 136 measurements, labeling offset = 90 mm, labeling duration = 2.1 seconds, and post-labeling delay = 0.93 seconds. In total, 68 alternating labeled and unlabeled image pairs were collected. Equilibrium magnetization (M<sub>0</sub>) images were collected using a long TR = 10-second protocol. Labeled and unlabeled pCASL images were independently motion corrected and a combined mean image was computed and coregistered to the spatially normalized T1W anatomical image. Perfusion-weighted images were calculated by voxel-wise subtractions of labeled and unlabeled images resulting in a mean perfusion-weighted image. Absolute WM perfusion or WM CBF (blood flow and perfusion are interchangeable terms here) quantification was calculated in native space from the mean perfusion images. Voxel-wise perfusion, in mL per 100 g/min, was calculated under the assumption that the post-label delay was longer than average transfer time, where labeling efficiency was set at 0.99 and the mean transit time was set to 0.7 seconds based on empirical data. The data collection preceded the publication and was not based on the consensus guidelines for ASL-in-dementia parameters [8]. Instead, the imaging parameters were derived empirically to maximize detection of WM perfusion by increasing labeling efficiency and SNR. In short, pCASL data in five healthy volunteers, representative of the study population (average age  $25.1 \pm 6.4$  range 20-35 years), were collected using the range of the labeling offset distances, labeling duration, and post-labeling delay times. Least-square fitting was used to calculate the sequence parameters that maximized the labeling efficiency across cerebral WM in all five subjects. This ensured that the derived parameters take into account the geometry of the MRI scanner and incorporate vascular physiology aspects of the subjects in this sample.

Proton MRS data were acquired from voxels placed in frontal WM and the anterior cingulate (AC). For the frontal WM region, short TE and long TE data were acquired using point resolved spectroscopy localization (TR = 1500 ms, short TE = 30, long TE = 135 ms, number of excitations averaged (NEX) = 256, 1.2-kHz spectral width, 1024 complex points, volume of interest  $\sim 3.4$  cm<sup>3</sup>). Data were acquired in both hemispheres and averaged together. For the AC, the same short TE point resolved spectroscopy localization parameters were used with a voxel size of 6 cm<sup>3</sup>. A water reference (NEX = 8) was also acquired for all datasets to be used for phase and eddy current correction. A basis set of 19 metabolites was simulated using the gamma visual analysis (GAVA) software for use in quantifying the 30-ms TE MRS data: alanine, aspartate, creatine (Cr),  $\gamma$ -aminobutyric acid, glucose, glutamate (Glu), glutamine (Gln), glutathione (GSH), glycine, glycerophosphocholine, lactate, myo-inositol (mI), N-acetylaspartate (NAA), N-acetylaspartylglutamate, phosphocholine, phosphocreatine, phosphoroylethanolamine, scyllo-inositol, and taurine. A basis set of eight metabolites simulated using the same software package was generated for use in quantifying 135-ms TE data: Cr, glycerophosphocholine, lactate, mI, NAA, N-acetylaspartylglutamate, phosphocholine, and phosphocreatine. Each basis set was imported into LCModel (6.3-0I) and used for quantification. Metabolite levels were reported in institutional units, and all metabolites with percent standard deviation Cramer-Rao lower bounds  $\leq 20\%$  were included in statistical analyses. One subject's MRI#1 and one subject's MRI#2 were excluded due to excessive artifact. As the AC region is a mixture of GM and WM, AC metabolite levels were corrected for the proportion of the GM, WM, and cerebrospinal fluid (CSF) within the spectroscopic voxel using in-house Matlab code based directly on the work of Gasparovic [9]. More specifically, tissue segmentation was performed in Statistical Parametric

Mapping 8 using the T1W images acquired for voxel positioning to obtain the fraction of GM, WM, and CSF.

#### **4.4 Statistical Analysis**

We utilized the freely available R Project for Statistical Computing functions of generalized linear model (GLM), Kolmogorov-Smirnov (KS), Wilcoxon rank test, t-test, and Pearson's correlation for statistical relevance. For GLM calculations, we used subjects' age as a nuisance covariate. We selected the KS test as our primary test, as it is a more conservative statistical test for comparison of FA values; GLM was more liberal and tended to demonstrate overall more significant  $p$ -values. We used the Wilcoxon rank sum test for comparison of nonparametric WMH burden, and we used the t-test for comparison of neurocognitive testing results. We also used Pearson's correlation test for comparison of neurocognitive to FA results. We considered  $p \leq 0.05$  as significant. We applied the Bonferroni multiple test correction for determination of by-tract significance and considered the Bonferroni adjusted  $p \leq 0.05$  as significant.

### **5.0 RESULTS**

#### **5.1 Overall Limitations/Challenges**

Laboratory evaluation with regard to microparticles at the University of Maryland remained inconsistent among individuals even after resolving consistency in shipping methods from the Lackland WHASC laboratory. Handling of the microparticle samples and processing of shipments were not consistent, as presumed in a certified lab. Even after correction and standardization, microparticle markers did not show significant changes or trends and were discontinued.

Inflammatory marker data also did not show significant findings, which we believe was secondary to the process used by LabCorp, as it is designed for clinical use and not research use. For the follow-on "phase 3" study we will use new inflammatory marker multiplex evaluation technology at the 59<sup>th</sup> Clinical Research Division.

#### **5.2 Reproducibility of Quantitative Structural and Physiological MRI Measurements**

We separated measurements into structural and physiological. Structural measurements included cortical GM thickness, FLAIR WMH volume and count, DTI-FA, and multi- $b$ -value diffusion imaging (MBI). Physiological measurements included CBF and concentrations of neurochemicals. In general, structural measurements demonstrated greater consistency than physiological measurements (Tables 1-7).

Mean coefficient of variation (MCV), mean relative difference (MRD), and intraclass correlation (ICC) for subcortical WMH volume/count on FLAIR showed better consistency compared to periependymal WMH volume and count in terms of higher ICCs (Table 1; ICC range 0.465–0.998). In terms of volume, MCVs and MRDs for subcortical and periependymal WMH volume were comparable. In terms of number of lesions, subcortical lesion count reproducibility was better than periependymal lesion count as evidenced by lower MCV and MRD values. Whole-brain cortical GM thickness was highly consistent, while individual

segments had more variability, with entorhinal, insula, and medial orbitofrontal being the least consistent in terms of ICC (Table 2; ICC range 0.747–0.987). All measurements were high or moderate on the 3% and high on the 10% reproducibility rating scale. MCV, MRD, and ICC for whole-brain global FA had excellent reproducibility, while individual tracts varied in consistency (Table 3; ICC range 0.865–0.979). The least consistent tracts were the fornix (FX), CS, and FO as evidenced by the highest MCV and MRD values and lowest ICCs. MBI (commonly referred to as q-space) was more consistent in the CC than AC, with  $M_u$  more consistent than PDI (Table 4; ICC range 0.434–0.967). All measurements were high on the 3% and 10% reproducibility rating scale.

**Table 1. Consistency of FLAIR**

| Volume and Count             | V1 Mean<br>[95% CI] <sup>a</sup> | V2 Mean<br>[95% CI] <sup>a</sup> | MCV (%)<br>[95% CI] | MRD (%)<br>[95% CI] | ICC<br>3% <sup>b</sup> | Rating                     | Rating<br>10% <sup>b</sup> |
|------------------------------|----------------------------------|----------------------------------|---------------------|---------------------|------------------------|----------------------------|----------------------------|
| Total volume                 | 0.15 [0.12, 6.48]                | 0.14 [0.11, 01.7]                | 7.8 [4.9, 10.8]     | 10.4 [6.7, 14.1]    | 0.981                  | <i>N</i> =35<br>(moderate) | <i>N</i> =4<br>(high)      |
| Total lesions                | 4.82 [3.16, 6.48]                | 4.68 [3.04, 6.33]                | 7.1 [2.6, 11.6]     | 10.2 [3.7, 16.7]    | 0.989<br>(low)         | <i>N</i> =130              | <i>N</i> =13<br>(high)     |
| Subcortical volume           | 0.024 [0.011, 0.038]             | 0.025 [0.010, 0.040]             | 9.2 [4.2, 14.3]     | 14.0 [5.2, 22.9]    | 0.994                  | <i>N</i> =38<br>(moderate) | <i>N</i> =5<br>(high)      |
| Periependymal volume         | 0.13 [0.10, 0.15]                | 0.12 [0.095, 0.14]               | 9.1 [6.2, 12.0]     | 12.1 [8.5, 15.8]    | 0.974<br>(low)         | <i>N</i> =41               | <i>N</i> =5<br>(high)      |
| Subcortical number lesions   | 2.41 [0.778, 4.04]               | 2.36 [0.76, 4.00]                | 3.6 [-0.92, 8.2]    | 6.7 [-2.6, 16.1]    | 0.998                  | <i>N</i> =39<br>(moderate) | <i>N</i> =5<br>(high)      |
| Periependymal number lesions | 2.41 [2.16, 2.66]                | 2.32 [2.08, 2.56]                | 9.5 [3.3, 15.7]     | 12.9 [4.6, 21.2]    | 0.465<br>(low)         | <i>N</i> =277              | <i>N</i> =26<br>(high)     |

CI = confidence interval [lower limit, upper limit].

<sup>a</sup>*N*=22.

<sup>b</sup>Reproducibility rating for 10% detection, power = 0.9, and significance = 0.05.

**Table 2. Consistency of Cortical Thickness**

| Segment                   | V1 Mean<br>[95% CI] <sup>a</sup> | V2 Mean<br>[95% CI] <sup>a</sup> | V3 Mean<br>[95% CI] <sup>b</sup> | MCV (%)<br>[95% CI] | MRD (%)<br>[95% CI] | Rating |                        | Rating<br>10% <sup>c</sup> |
|---------------------------|----------------------------------|----------------------------------|----------------------------------|---------------------|---------------------|--------|------------------------|----------------------------|
|                           |                                  |                                  |                                  |                     |                     | ICC    | 3% <sup>c</sup>        |                            |
| Whole-brain GM            | 2.67 [2.62, 2.71]                | 2.66 [2.62, 2.70]                | 2.67 [2.62, 2.71]                | 0.80 [0.61, 0.98]   | 1.1 [0.80, 1.3]     | 0.980  | <i>N</i> =3<br>(high)  | <i>N</i> =2<br>(high)      |
| <i>Left Hemisphere</i>    |                                  |                                  |                                  |                     |                     |        |                        |                            |
| Mean thickness            | 2.67 [2.62, 2.72]                | 2.66 [2.62, 2.70]                | 2.67 [2.62, 2.71]                | 0.88 [0.64, 1.0]    | 1.2 [0.92, 1.4]     | 0.979  | <i>N</i> =3<br>(high)  | <i>N</i> =2<br>(high)      |
| BanksSTS                  | 2.64 [2.57, 2.71]                | 2.64 [2.59, 2.70]                | 2.64 [2.57, 2.70]                | 2.1 [1.6, 2.5]      | 2.7 [2.1, 3.2]      | 0.940  | <i>N</i> =11<br>(high) | <i>N</i> =2<br>(high)      |
| Caudal anterior cingulate | 2.77 [2.68, 2.86]                | 2.73 [2.63, 2.83]                | 2.74 [2.63, 2.84]                | 2.6 [1.9, 3.2]      | 3.3 [2.5, 4.1]      | 0.959  | <i>N</i> =17<br>(high) | <i>N</i> =3<br>(high)      |
| Caudal middle frontal     | 2.74 [2.68, 2.79]                | 2.72 [2.67, 2.77]                | 2.71 [2.66, 2.77]                | 1.3 [1.0, 1.7]      | 1.7 [1.3, 2.1]      | 0.957  | <i>N</i> =5<br>(high)  | <i>N</i> =2<br>(high)      |
| Cuneus                    | 1.99 [1.92, 2.06]                | 2.03 [1.96, 2.10]                | 2.02 [1.95, 2.09]                | 2.4 [1.7, 3.1]      | 3.2 [2.2, 4.2]      | 0.962  | <i>N</i> =13<br>(high) | <i>N</i> =3<br>(high)      |
| Entorhinal                | 3.59 [3.49, 3.70]                | 3.51 [3.41, 3.62]                | 3.56 [3.46, 3.65]                | 3.9 [3.0, 4.8]      | 5.0 [3.9, 6.1]      | 0.747  | <i>N</i> =42<br>(low)  | <i>N</i> =5<br>(high)      |
| Fusiform                  | 2.88 [2.83, 2.94]                | 2.87 [2.81, 2.93]                | 2.87 [2.81, 2.93]                | 1.3 [1.0, 1.5]      | 1.6 [1.3, 1.9]      | 0.889  | <i>N</i> =5<br>(high)  | <i>N</i> =2<br>(high)      |
| Inferior parietal         | 2.63 [2.57, 2.68]                | 2.63 [2.58, 2.67]                | 2.64 [2.58, 2.70]                | 1.1 [0.85, 1.4]     | 1.5 [1.1, 1.8]      | 0.977  | <i>N</i> =4<br>(high)  | <i>N</i> =2<br>(high)      |
| Inferior temporal         | 3.01 [2.94, 3.07]                | 3.01 [2.95, 3.07]                | 3.01 [2.95, 3.08]                | 1.4 [1.1, 1.7]      | 1.8 [1.5, 2.2]      | 0.967  | <i>N</i> =6<br>(high)  | <i>N</i> =2<br>(high)      |
| Isthmus cingulate         | 2.54 [2.46, 2.61]                | 2.54 [2.46, 2.62]                | 2.51 [2.43, 2.60]                | 2.4 [2.0, 2.9]      | 3.1 [2.6, 3.7]      | 0.950  | <i>N</i> =15<br>(high) | <i>N</i> =3<br>(high)      |
| Lateral occipital         | 2.28 [2.22, 2.33]                | 2.28 [2.22, 2.34]                | 2.30 [2.24, 2.36]                | 1.6 [1.1, 2.0]      | 2.1 [1.5, 2.7]      | 0.966  | <i>N</i> =7<br>(high)  | <i>N</i> =2<br>(high)      |
| Lateral orbitofrontal     | 2.92 [2.85, 2.98]                | 2.90 [2.83, 2.96]                | 2.87 [2.80, 2.95]                | 1.9 [1.5, 2.3]      | 2.4 [1.7, 3.0]      | 0.955  | <i>N</i> =9<br>(high)  | <i>N</i> =2<br>(high)      |
| Lingual                   | 2.21 [2.15, 2.27]                | 2.21 [2.15, 2.27]                | 2.21 [2.15, 2.28]                | 1.8 [1.3, 2.3]      | 2.3 [1.7, 3.0]      | 0.974  | <i>N</i> =8<br>(high)  | <i>N</i> =2<br>(high)      |

**Table 2. Consistency of Cortical Thickness (continued)**

| Segment                    | V1 Mean<br>[95% CI] <sup>a</sup> | V2 Mean<br>[95% CI] <sup>a</sup> | V3 Mean<br>[95% CI] <sup>b</sup> | MCV (%)<br>[95% CI] | MRD (%)<br>[95% CI] | Rating |                    | Rating<br>10% <sup>c</sup> |
|----------------------------|----------------------------------|----------------------------------|----------------------------------|---------------------|---------------------|--------|--------------------|----------------------------|
|                            |                                  |                                  |                                  |                     |                     | ICC    | 3% <sup>c</sup>    |                            |
| Medial orbitofrontal       | 2.72 [2.65, 2.79]                | 2.70 [2.63, 2.76]                | 2.68 [2.61, 2.75]                | 3.0 [2.5, 3.5]      | 3.9 [3.3, 4.5]      | 0.898  | N=21<br>(moderate) | N=3<br>(high)              |
| Middle temporal            | 3.10 [3.03, 3.17]                | 3.08 [3.01, 3.14]                | 3.10 [3.03, 3.16]                | 1.1 [0.78, 1.4]     | 1.4 [1.0, 1.8]      | 0.977  | N=4<br>(high)      | N=2<br>(high)              |
| Parahippocampal            | 2.83 [2.70, 2.96]                | 2.80 [2.67, 2.93]                | 2.80 [2.66, 2.93]                | 2.2 [1.9, 2.5]      | 2.8 [2.4, 3.3]      | 0.984  | N=13<br>(high)     | N=3<br>(high)              |
| Paracentral                | 2.53 [2.48, 2.59]                | 2.54 [2.49, 2.59]                | 2.56 [2.50, 2.62]                | 1.4 [1.4, 1.8]      | 1.8 [1.4, 2.2]      | 0.964  | N=6<br>(high)      | N=2<br>(high)              |
| Parsopercularis            | 2.85 [2.80, 2.91]                | 2.85 [2.80, 2.90]                | 2.85 [2.78, 2.91]                | 0.97 [0.74, 1.2]    | 1.3 [0.97, 1.5]     | 0.980  | N=3<br>(high)      | N=2<br>(high)              |
| Parsorbitalis              | 3.01 [2.94, 3.07]                | 2.98 [2.92, 3.04]                | 3.04 [2.97, 3.11]                | 1.8 [1.3, 2.4]      | 2.3 [1.6, 3.1]      | 0.963  | N=8<br>(high)      | N=2<br>(high)              |
| Parstriangularis           | 2.73 [2.67, 2.80]                | 2.71 [2.65, 2.77]                | 2.71 [2.64, 2.78]                | 1.3 [1.0, 1.6]      | 1.6 [1.3, 2.0]      | 0.981  | N=5<br>(high)      | N=2<br>(high)              |
| Pericalcarine              | 1.76 [1.69, 1.83]                | 1.80 [1.72, 1.88]                | 1.79 [1.72, 1.86]                | 2.7 [2.0, 3.4]      | 3.5 [2.6, 4.4]      | 0.978  | N=17<br>(high)     | N=3<br>(high)              |
| Postcentral                | 2.20 [2.15, 2.25]                | 2.20 [2.16, 2.25]                | 2.20 [2.15, 2.25]                | 1.2 [0.90, 1.5]     | 1.6 [1.2, 2.0]      | 0.972  | N=5<br>(high)      | N=2<br>(high)              |
| Posterior cingulate        | 2.60 [2.54, 2.65]                | 2.60 [2.54, 2.65]                | 2.58 [2.52, 2.64]                | 1.4 [1.1, 1.7]      | 1.9 [1.4, 2.3]      | 0.957  | N=6<br>(high)      | N=2<br>(high)              |
| Precentral                 | 2.73 [2.69, 2.77]                | 2.72 [2.68, 2.75]                | 2.73 [2.69, 2.77]                | 1.0 [0.73, 1.3]     | 1.3 [0.96, 1.6]     | 0.951  | N=4<br>(high)      | N=2<br>(high)              |
| Precuneus                  | 2.55 [2.49, 2.60]                | 2.54 [2.49, 2.60]                | 2.55 [2.50, 2.61]                | 0.98 [0.75, 1.2]    | 1.3 [0.97, 1.6]     | 0.983  | N=4<br>(high)      | N=2<br>(high)              |
| Rostral anterior cingulate | 3.06 [2.95, 3.17]                | 3.02 [2.89, 3.15]                | 3.02 [2.89, 3.15]                | 3.0 [2.2, 3.9]      | 3.9 [2.8, 5.0]      | 0.952  | N=21<br>(moderate) | N=3<br>(high)              |
| Rostral middle frontal     | 2.62 [2.56, 2.60]                | 2.60 [2.54, 2.65]                | 2.59 [2.52, 2.66]                | 1.5 [1.2, 1.9]      | 2.0 [1.6, 2.4]      | 0.971  | N=6<br>(high)      | N=2<br>(high)              |
| Superior frontal           | 2.86 [2.81, 2.91]                | 2.84 [2.79, 2.88]                | 2.86 [2.82, 2.91]                | 1.6 [1.1, 2.1]      | 2.0 [1.4, 2.7]      | 0.918  | N=7<br>(high)      | N=2<br>(high)              |
| Superior parietal          | 2.30 [2.24, 2.35]                | 2.31 [2.26, 2.35]                | 2.31 [2.26, 2.36]                | 1.1 [0.84, 1.4]     | 1.4 [1.1, 1.7]      | 0.980  | N=4<br>(high)      | N=2<br>(high)              |
| Superior temporal          | 3.05 [2.99, 3.11]                | 3.05 [2.99, 3.11]                | 3.07 [3.00, 3.14]                | 1.2 [0.87, 1.5]     | 1.5 [1.1, 1.9]      | 0.970  | N=4<br>(high)      | N=2<br>(high)              |
| Supramarginal              | 2.75 [2.69, 2.81]                | 2.75 [2.70, 2.81]                | 2.75 [2.69, 2.82]                | 1.0 [0.83, 1.2]     | 1.3 [1.1, 1.6]      | 0.983  | N=4<br>(high)      | N=2<br>(high)              |
| Frontal pole               | 3.10 [2.99, 3.21]                | 3.12 [3.01, 3.24]                | 3.13 [3.01, 3.25]                | 3.2 [2.1, 4.3]      | 4.3 [2.8, 5.8]      | 0.918  | N=23<br>(moderate) | N=3<br>(high)              |
| Temporal pole              | 3.97 [3.88, 4.06]                | 3.97 [3.89, 4.06]                | 3.91 [3.81, 4.02]                | 2.2 [1.7, 2.8]      | 2.9 [2.2, 3.6]      | 0.919  | N=12<br>(high)     | N=2<br>(high)              |
| Transverse temporal        | 2.67 [2.57, 2.78]                | 2.70 [2.60, 2.79]                | 2.69 [2.60, 2.79]                | 2.0 [1.5, 2.6]      | 2.6 [2.0, 3.3]      | 0.971  | N=11<br>(high)     | N=2<br>(high)              |
| Insula                     | 3.22 [3.15, 3.28]                | 3.24 [3.18, 3.30]                | 3.23 [3.17, 3.29]                | 2.2 [1.6, 2.8]      | 2.9 [2.1, 3.7]      | 0.890  | N=12<br>(high)     | N=2<br>(high)              |
| <b>Right Hemisphere</b>    |                                  |                                  |                                  |                     |                     |        |                    |                            |
| Mean thickness             | 2.67 [2.62, 2.71]                | 2.66 [2.62, 2.70]                | 2.66 [2.62, 2.71]                | 0.83 [0.64, 1.0]    | 1.1 [0.84, 1.4]     | 0.978  | N=3<br>(high)      | N=2<br>(high)              |
| BanksSTS                   | 2.81 [2.75, 2.87]                | 2.80 [2.75, 2.86]                | 2.76 [2.70, 2.82]                | 1.4 [1.2, 1.7]      | 1.9 [1.5, 2.2]      | 0.967  | N=6<br>(high)      | N=2<br>(high)              |
| Caudal anterior cingulate  | 2.66 [2.58, 2.74]                | 2.65 [2.59, 2.72]                | 2.67 [2.58, 2.75]                | 2.3 [1.9, 2.7]      | 3.0 [2.4, 3.5]      | 0.948  | N=14<br>(high)     | N=3<br>(high)              |
| Caudal middle frontal      | 2.65 [2.60, 2.70]                | 2.65 [2.60, 2.70]                | 2.64 [2.59, 2.69]                | 1.3 [0.99, 1.6]     | 1.7 [1.3, 2.1]      | 0.958  | N=5<br>(high)      | N=2<br>(high)              |
| Cuneus                     | 2.03 [1.96, 2.09]                | 2.05 [1.98, 2.12]                | 2.03 [1.96, 2.12]                | 2.1 [1.4, 2.9]      | 2.7 [1.9, 3.6]      | 0.960  | N=11<br>(high)     | N=2<br>(high)              |
| Entorhinal                 | 3.61 [3.52, 3.70]                | 3.56 [3.46, 3.66]                | 3.66 [3.55, 3.78]                | 4.2 [3.3, 5.1]      | 5.6 [4.3, 6.8]      | 0.781  | N=42<br>(low)      | N=5<br>(high)              |
| Fusiform                   | 2.89 [2.84, 2.94]                | 2.88 [2.83, 2.93]                | 2.86 [2.81, 2.92]                | 1.4 [1.1, 1.8]      | 1.8 [1.4, 2.3]      | 0.961  | N=6<br>(high)      | N=2<br>(high)              |
| Inferior parietal          | 2.66 [2.59, 2.72]                | 2.65 [2.60, 2.71]                | 2.66 [2.60, 2.73]                | 1.2 [0.95, 1.4]     | 1.5 [1.2, 1.8]      | 0.978  | N=5<br>(high)      | N=2<br>(high)              |
| Inferior temporal          | 3.04 [2.99, 3.10]                | 3.04 [2.97, 3.10]                | 3.03 [2.96, 3.10]                | 1.5 [1.1, 1.9]      | 1.9 [1.4, 2.4]      | 0.963  | N=6<br>(high)      | N=2<br>(high)              |
| Isthmus cingulate          | 2.44 [2.40, 2.49]                | 2.46 [2.40, 2.52]                | 2.45 [2.39, 2.51]                | 2.1 [1.6, 2.5]      | 2.7 [2.0, 3.3]      | 0.931  | N=11<br>(high)     | N=2<br>(high)              |

**Table 2. Consistency of Cortical Thickness (concluded)**

| Segment                    | V1 Mean<br>[95% CI] <sup>a</sup> | V2 Mean<br>[95% CI] <sup>a</sup> | V3 Mean<br>[95% CI] <sup>b</sup> | MCV (%)<br>[95% CI] | MRD (%)<br>[95% CI] | Rating |                    | Rating<br>10% <sup>c</sup> |
|----------------------------|----------------------------------|----------------------------------|----------------------------------|---------------------|---------------------|--------|--------------------|----------------------------|
|                            |                                  |                                  |                                  |                     |                     | ICC    | 3% <sup>c</sup>    |                            |
| Lateral occipital          | 2.31 [2.25, 2.38]                | 2.31 [2.25, 2.38]                | 2.33 [2.26, 2.40]                | 1.7 [1.3, 2.1]      | 2.2 [1.6, 2.8]      | 0.976  | N=8<br>(high)      | N=2<br>(high)              |
| Lateral orbitofrontal      | 2.88 [2.82, 2.94]                | 2.88 [2.83, 2.92]                | 2.85 [2.79, 2.92]                | 2.0 [1.6, 2.5]      | 2.6 [2.1, 3.2]      | 0.901  | N=11<br>(high)     | N=2<br>(high)              |
| Lingual                    | 2.29 [2.24, 2.35]                | 2.31 [2.25, 2.38]                | 2.31 [2.25, 2.37]                | 1.6 [1.2, 2.0]      | 2.1 [1.6, 2.6]      | 0.977  | N=7<br>(high)      | N=2<br>(high)              |
| Medial orbitofrontal       | 2.77 [2.72, 2.83]                | 2.76 [2.69, 2.82]                | 2.73 [2.67, 2.79]                | 2.0 [1.5, 2.6]      | 2.6 [1.9, 3.3]      | 0.882  | N=12<br>(high)     | N=2<br>(high)              |
| Middle temporal            | 3.17 [3.11, 3.23]                | 3.15 [3.09, 3.21]                | 3.14 [3.07, 3.21]                | 1.3 [1.1, 1.6]      | 1.7 [1.4, 2.1]      | 0.972  | N=5<br>(high)      | N=2<br>(high)              |
| Parahippocampal            | 2.78 [2.67, 2.89]                | 2.76 [2.63, 2.89]                | 2.76 [2.63, 2.88]                | 2.2 [1.1, 2.8]      | 2.8 [2.1, 3.5]      | 0.980  | N=12<br>(high)     | N=2<br>(high)              |
| Paracentral                | 2.56 [2.50, 2.61]                | 2.57 [2.51, 2.62]                | 2.57 [2.51, 2.62]                | 1.4 [1.2, 1.7]      | 1.9 [1.5, 2.2]      | 0.961  | N=6<br>(high)      | N=2<br>(high)              |
| Parsopercularis            | 2.80 [2.75, 2.85]                | 2.80 [2.75, 2.85]                | 2.79 [2.74, 2.84]                | 1.0 [0.76, 1.3]     | 1.3 [0.97, 1.7]     | 0.971  | N=4<br>(high)      | N=2<br>(high)              |
| Parsorbitalis              | 3.02 [2.94, 3.10]                | 3.03 [2.97, 3.08]                | 3.02 [2.95, 3.08]                | 1.8 [1.3, 2.3]      | 2.4 [1.7, 3.0]      | 0.953  | N=9<br>(high)      | N=2<br>(high)              |
| Parstriangularis           | 2.73 [2.66, 2.80]                | 2.72 [2.65, 2.78]                | 2.71 [2.64, 2.78]                | 1.5 [1.2, 1.8]      | 2.0 [1.6, 2.4]      | 0.970  | N=6<br>(high)      | N=2<br>(high)              |
| Pericalcarine              | 1.77 [1.70, 1.84]                | 1.80 [1.72, 1.89]                | 1.79 [1.71, 1.86]                | 2.8 [2.2, 3.4]      | 3.7 [2.9, 4.5]      | 0.967  | N=18<br>(high)     | N=3<br>(high)              |
| Postcentral                | 2.17 [2.12, 2.22]                | 2.19 [2.13, 2.24]                | 2.16 [2.10, 2.21]                | 1.5 [0.81, 2.2]     | 1.9 [1.1, 2.7]      | 0.929  | N=7<br>(high)      | N=2<br>(high)              |
| Posterior cingulate        | 2.62 [2.55, 2.68]                | 2.61 [2.54, 2.68]                | 2.60 [2.55, 2.66]                | 1.3 [0.87, 1.7]     | 1.7 [1.2, 2.2]      | 0.962  | N=5<br>(high)      | N=2<br>(high)              |
| Precentral                 | 2.69 [2.65, 2.73]                | 2.67 [2.63, 2.71]                | 2.68 [2.64, 2.72]                | 1.2 [0.70, 1.6]     | 1.5 [0.691, 2.0]    | 0.929  | N=4<br>(high)      | N=2<br>(high)              |
| Precuneus                  | 2.54 [2.48, 2.59]                | 2.54 [2.48, 2.59]                | 2.54 [2.48, 2.60]                | 1.0 [0.78, 1.1]     | 1.3 [1.0, 1.5]      | 0.985  | N=4<br>(high)      | N=2<br>(high)              |
| Rostral anterior cingulate | 3.12 [3.03, 3.21]                | 3.09 [3.00, 3.18]                | 3.09 [3.00, 3.19]                | 3.1 [2.3, 3.8]      | 3.9 [2.9, 4.8]      | 0.899  | N=23<br>(moderate) | N=3<br>(high)              |
| Rostral middle frontal     |                                  | 2.56 [2.52, 2.60]                | 2.56 [2.51, 2.60]                | 1.4 [1.1, 1.7]      | 1.8 [1.4, 2.2]      | 0.952  | N=5<br>(high)      | N=2<br>(high)              |
| Superior frontal           | 2.84 [2.78, 2.91]                | 2.82 [2.77, 2.87]                | 2.84 [2.78, 2.89]                | 1.7 [1.3, 2.1]      | 2.2 [1.7, 2.8]      | 0.937  | N=8<br>(high)      | N=2<br>(high)              |
| Superior parietal          | 2.32 [2.26, 2.37]                | 2.32 [2.27, 2.37]                | 2.32 [2.26, 2.37]                | 1.1 [0.92, 1.4]     | 1.5 [1.2, 1.8]      | 0.987  | N=4<br>(high)      | N=2<br>(high)              |
| Superior temporal          | 3.08 [3.01, 3.14]                | 3.07 [2.95, 3.19]                | 3.09 [3.02, 3.15]                | 1.1 [0.73, 1.4]     | 1.4 [0.95, 1.9]     | 0.980  | N=4<br>(high)      | N=2<br>(high)              |
| Supramarginal              | 2.74 [2.68, 2.80]                | 2.73 [2.68, 2.78]                | 2.72 [2.66, 2.79]                | 1.1 [0.83, 1.4]     | 1.4 [1.1, 1.8]      | 0.981  | N=4<br>(high)      | N=2<br>(high)              |
| Frontal pole               | 3.12 [2.99, 3.25]                | 3.07 [2.95, 3.19]                | 3.09 [2.96, 3.21]                | 3.2 [2.2, 4.1]      | 4.1 [2.8, 5.3]      | 0.940  | N=24<br>(moderate) | N=3<br>(high)              |
| Temporal pole              | 4.06 [3.96, 4.16]                | 4.01 [3.91, 4.11]                | 4.04 [3.93, 4.15]                | 2.3 [1.8, 2.9]      | 3.0 [2.3, 3.8]      | 0.921  | N=14<br>(high)     | N=3<br>(high)              |
| Transverse temporal        | 2.70 [2.61, 2.79]                | 2.71 [2.60, 2.81]                | 2.69 [2.59, 2.79]                | 2.3 [1.6, 3.0]      | 2.9 [2.1, 3.7]      | 0.969  | N=13<br>(high)     | N=3<br>(high)              |
| Insula                     | 3.20 [3.14, 3.25]                | 3.15 [3.10, 3.20]                | 3.19 [3.13, 3.26]                | 2.4 [1.8, 2.9]      | 3.1 [2.4, 3.8]      | 0.809  | N=14<br>(high)     | N=3<br>(high)              |

BanksSTS = region around superior temporal sulcus.

<sup>a</sup>N=25.

<sup>b</sup>N=22.

<sup>c</sup>Reproducibility rating for 10% detection, power = 0.9, and significance = 0.05.

**Table 3. Consistency of FA Derived from DTI**

| Tract       | V1 Mean<br>[95% CI] <sup>a</sup> | V2 Mean<br>[95% CI] <sup>a</sup> | V3 Mean<br>[95% CI] <sup>b</sup> | MCV (%)<br>[95% CI] | MRD (%)<br>[95% CI] | ICC   | Rating<br>3% <sup>c</sup> | Rating<br>10% <sup>c</sup> |
|-------------|----------------------------------|----------------------------------|----------------------------------|---------------------|---------------------|-------|---------------------------|----------------------------|
| Avg         | 0.50 [0.49, 0.51]                | 0.50 [0.49, 0.51]                | 0.50 [0.49, 0.51]                | 0.91 [0.51, 1.3]    | 1.2 [0.63, 1.8]     | 0.979 | N=3<br>(high)             | N=2<br>(high)              |
| Genu        | 0.74 [0.73, 0.76]                | 0.74 [0.73, 0.76]                | 0.75 [0.73, 0.76]                | 0.99 [0.69, 1.3]    | 1.3 [0.90, 1.7]     | 0.964 | N=4<br>(high)             | N=2<br>(high)              |
| Body        | 0.73 [0.71, 0.74]                | 0.73 [0.71, 0.74]                | 0.73 [0.71, 0.75]                | 1.6 [1.0, 2.1]      | 2.0 [1.3, 2.7]      | 0.965 | N=6<br>(high)             | N=2<br>(high)              |
| Splenium    | 0.84 [0.83, 0.85]                | 0.84 [0.83, 0.85]                | 0.84 [0.82, 0.85]                | 0.88 [0.58, 1.1]    | 1.1 [0.76, 1.5]     | 0.969 | N=3<br>(high)             | N=2<br>(high)              |
| FX          | 0.55 [0.53, 0.56]                | 0.55 [0.54, 0.57]                | 0.55 [0.53, 0.57]                | 3.8 [2.5, 5.2]      | 5.0 [3.1, 6.9]      | 0.865 | N=30<br>(moderate)        | N=4<br>(high)              |
| CS          | 0.70 [0.68, 0.72]                | 0.71 [0.69, 0.73]                | 0.71 [0.69, 0.72]                | 2.8 [1.6, 3.9]      | 3.8 [2.0, 5.5]      | 0.910 | N=21<br>(moderate)        | N=3<br>(high)              |
| IC          | 0.68 [0.67, 0.69]                | 0.68 [0.67, 0.70]                | 0.68 [0.67, 0.70]                | 1.6 [0.86, 2.2]     | 2.1 [1.1, 3.1]      | 0.942 | N=5<br>(high)             | N=2<br>(high)              |
| CR          | 0.53 [0.52, 0.54]                | 0.53 [0.52, 0.54]                | 0.53 [0.52, 0.54]                | 1.5 [1.0, 1.9]      | 1.9 [1.3, 2.6]      | 0.967 | N=5<br>(high)             | N=2<br>(high)              |
| Tr          | 0.67 [0.66, 0.68]                | 0.67 [0.66, 0.68]                | 0.67 [0.65, 0.68]                | 1.2 [0.77, 1.7]     | 1.6 [0.96, 2.2]     | 0.960 | N=4<br>(high)             | N=2<br>(high)              |
| SS          | 0.61 [0.60, 0.62]                | 0.61 [0.60, 0.63]                | 0.61 [0.59, 0.62]                | 1.6 [1.1, 2.1]      | 2.1 [1.4, 3.3]      | 0.965 | N=5<br>(high)             | N=2<br>(high)              |
| EC          | 0.54 [0.53, 0.55]                | 0.54 [0.53, 0.56]                | 0.54 [0.53, 0.55]                | 1.8 [1.2, 2.4]      | 2.4 [1.5, 3.3]      | 0.934 | N=7<br>(high)             | N=2<br>(high)              |
| Cing        | 0.68 [0.67, 0.70]                | 0.69 [0.67, 0.70]                | 0.69 [0.67, 0.71]                | 2.0 [1.4, 2.6]      | 2.7 [1.7, 3.6]      | 0.955 | N=9<br>(high)             | N=2<br>(high)              |
| SLF         | 0.55 [0.54, 0.56]                | 0.55 [0.54, 0.56]                | 0.55 [0.54, 0.56]                | 1.7 [1.3, 2.2]      | 2.3 [1.6, 3.0]      | 0.952 | N=7<br>(high)             | N=2<br>(high)              |
| FO          | 0.59 [0.58, 0.60]                | 0.59 [0.58, 0.61]                | 0.59 [0.58, 0.61]                | 2.5 [1.6, 3.4]      | 3.4 [2.0, 4.7]      | 0.882 | N=12<br>(high)            | N=2<br>(high)              |
| Superior FO | 0.59 [0.58, 0.61]                | 0.60 [0.58, 0.62]                | 0.60 [0.59, 0.62]                | 3.3 [2.3, 4.4]      | 4.5 [2.9, 6.1]      | 0.874 | N=21<br>(moderate)        | N=3<br>(high)              |
| Inferior FO | 0.58 [0.57, 0.60]                | 0.59 [0.57, 0.60]                | 0.59 [0.57, 0.60]                | 2.4 [1.5, 3.2]      | 3.2 [2.0, 4.3]      | 0.917 | N=13<br>(high)            | N=3<br>(high)              |

<sup>a</sup>N=25.

<sup>b</sup>N=21 (three subjects only completed two visits and one dataset removed due to artifact).

<sup>c</sup>Reproducibility rating for 10% detection, power = 0.9, and significance = 0.05.

**Table 4. Consistency of MBI (or q-space) for Corpus Callosum and Anterior Cingulate**

| Tract                     | V1 Mean<br>[95% CI] <sup>a</sup> | V2 Mean<br>[95% CI] <sup>a</sup> | V3 Mean<br>[95% CI] <sup>b</sup> | MCV (%)<br>[95% CI] | MRD (%)<br>[95% CI] | ICC   | Rating<br>3% <sup>c</sup> | Rating<br>10% <sup>c</sup> |
|---------------------------|----------------------------------|----------------------------------|----------------------------------|---------------------|---------------------|-------|---------------------------|----------------------------|
| <i>Corpus Callosum</i>    |                                  |                                  |                                  |                     |                     |       |                           |                            |
| CC $M_u$                  | 0.53 [0.51, 0.54]                | 0.52 [0.51, 0.54]                | 0.52 [0.51, 0.54]                | 2.1 [1.5, 2.7]      | 2.6 [1.8, 4.4]      | 0.967 | N=11<br>(high)            | N=2<br>(high)              |
| CC PDI                    | 0.037 [0.034, 0.041]             | 0.038 [0.034, 0.042]             | 0.038 [0.033, 0.042]             | 11.1 [7.8, 14.4]    | 13.8 [9.2, 23.0]    | 0.911 | N=28<br>(moderate)        | N=4<br>(high)              |
| <i>Anterior Cingulate</i> |                                  |                                  |                                  |                     |                     |       |                           |                            |
| AC $M_u$                  | 0.67 [0.66, 0.69]                | 0.66 [0.65, 0.68]                | 0.68 [0.66, 0.69]                | 4.0 [2.9, 5.1]      | 5.2 [3.8, 6.7]      | 0.434 | N=37<br>(moderate)        | N=4<br>(high)              |
| AC PDI                    | 0.047 [0.036, 0.058]             | 0.050 [0.040, 0.060]             | 0.040 [0.031, 0.049]             | 29.8 [21.3, 38.4]   | 39.8 [26.1, 53.8]   | 0.646 | N=240<br>(low)            | N=2<br>(moderate)          |

<sup>a</sup>N=25.

<sup>b</sup>N=22 (three subjects completed only two visits).

<sup>c</sup>Reproducibility rating for 10% detection, power = 0.9, and significance = 0.05.

MCV, MRD, and ICC for whole-brain GM pCASL were consistent, while individual segments varied, with greatest variability in the inferior temporal gyrus anterior, subcallosal cortex, cingulate gyrus anterior, parahippocampus gyrus anterior, and temporal fusiform cortex, posterior division (Table 5; ICC range 0.885–0.971). Whole-brain WM pCASL was also consistent, with again more variability in individual regions. The regions of greatest variability were the FX and CS (Table 6; ICC range 0.872–0.982). Most measurements were low on the 3% and 10% reproducibility rating scale with some exceptions. GM average CBF was moderate at 10%, while WM was high at both 3% and 10%. Other WM values had high or moderate reproducibility rating at 10% except for the FX, CS, and FO.

**Table 5. Consistency of GM Blood Flow as Measured by pCASL**

| Segment  | V1 Mean<br>[95% CI] <sup>a</sup> | V2 Mean<br>[95% CI] <sup>a</sup> | V3 Mean<br>[95% CI] <sup>b</sup> | MCV (%)<br>[95% CI] | MRD (%)<br>[95% CI] | ICC   | Rating<br>3% <sup>c</sup> | Rating<br>10% <sup>c</sup> |
|--|----------------------------------|----------------------------------|----------------------------------|---------------------|---------------------|-------|---------------------------|----------------------------|
| Avg CBF  | 51.8 [48.2, 55.4]                | 52.8 [49.1, 56.5]                | 50.9 [47.3, 54.6]                | 4.5 [3.3, 5.8]      | 5.8 [4.2, 7.4]      | 0.971 | N=45<br>(low)             | N=5<br>(high)              |
| Frontal pole                                       | 58.8 [54.6, 62.9]                | 59.0 [54.8, 63.2]                | 56.5 [52.2, 61.0]                | 6.6 [5.0, 8.2]      | 8.5 [6.3, 10.7]     | 0.954 | N=95<br>(low)             | N=10<br>(high)             |
| Insular cortex                                     | 45.7 [42.3, 49.1]                | 46.6 [43.3, 50.0]                | 43.7 [40.2, 47.3]                | 7.5 [6.0, 9.0]      | 9.6 [7.6, 11.6]     | 0.931 | N=124<br>(low)            | N=12<br>(high)             |
| Superior frontal gyrus                             | 68.7 [63.3, 74.1]                | 70.6 [65.4, 75.8]                | 67.3 [62.2, 72.5]                | 5.7 [4.2, 7.2]      | 7.5 [5.4, 9.6]      | 0.965 | N=69<br>(low)             | N=7<br>(high)              |
| Middle frontal gyrus                               | 67.7 [62.9, 72.5]                | 69.4 [64.5, 74.3]                | 65.6 [60.4, 70.9]                | 6.4 [5.1, 7.8]      | 8.3 [6.4, 10.2]     | 0.957 | N=91<br>(low)             | N=9<br>(high)              |
| Inferior frontal gyrus<br>parstriangularis         | 55.1 [51.4, 58.9]                | 56.7 [52.6, 60.8]                | 53.1 [48.9, 57.3]                | 7.1 [5.6, 8.6]      | 9.2 [7.2, 11.1]     | 0.939 | N=115<br>(low)            | N=11<br>(high)             |
| Inferior frontal gyrus<br>parsopercularis          | 56.5 [52.7, 60.3]                | 57.7 [53.8, 61.6]                | 55.2 [51.1, 59.4]                | 7.0 [5.7, 8.3]      | 8.9 [7.2, 10.7]     | 0.934 | N=109<br>(low)            | N=11<br>(high)             |
| Precentral gyrus                                   | 66.3 [61.5, 71.0]                | 68.4 [63.3, 73.4]                | 65.4 [60.6, 70.2]                | 5.6 [4.4, 7.0]      | 7.4 [5.6, 9.1]      | 0.960 | N=73<br>(low)             | N=8<br>(high)              |
| Temporal pole                                      | 42.1 [39.0, 45.2]                | 44.0 [40.8, 47.3]                | 40.4 [36.9, 43.8]                | 8.7 [7.0, 10.4]     | 11.1 [9.0, 13.2]    | 0.926 | N=167<br>(low)            | N=16<br>(high)             |
| Superior temporal gyrus,<br>anterior division      | 46.8 [42.9, 50.8]                | 47.3 [43.6, 50.9]                | 43.1 [39.7, 46.6]                | 9.1 [7.1, 11.1]     | 11.5 [9.1, 13.9]    | 0.901 | N=192<br>(low)            | N=18<br>(high)             |
| Superior temporal gyrus,<br>posterior division     | 53.6 [49.2, 58.0]                | 53.0 [48.9, 57.2]                | 50.2 [46.2, 54.2]                | 7.9 [6.3, 9.5]      | 10.1 [8.0, 12.1]    | 0.929 | N=142<br>(low)            | N=14<br>(high)             |
| Middle temporal gyrus,<br>anterior division        | 41.2 [38.1, 44.3]                | 42.7 [39.5, 46.0]                | 38.7 [35.1, 42.2]                | 8.9 [7.2, 10.7]     | 11.4 [9.2, 13.5]    | 0.931 | N=175<br>(low)            | N=17<br>(high)             |
| Middle temporal gyrus,<br>posterior division       | 46.7 [43.1, 50.4]                | 47.5 [43.7, 51.2]                | 43.9 [40.1, 47.7]                | 8.3 [6.6, 10.0]     | 10.5 [8.4, 12.7]    | 0.929 | N=156<br>(low)            | N=15<br>(high)             |
| Middle temporal gyrus,<br>temporo-occipital part   | 47.2 [43.7, 50.7]                | 48.5 [44.4, 52.6]                | 46.0 [42.2, 49.7]                | 7.6 [6.0, 9.2]      | 9.9 [7.8, 12.0]     | 0.925 | N=136<br>(low)            | N=13<br>(high)             |
| Inferior temporal gyrus,<br>anterior division      | 36.2 [33.0, 39.4]                | 37.1 [33.9, 40.2]                | 34.1 [30.7, 37.5]                | 10.1 [7.7, 12.6]    | 12.7 [10.0, 15.5]   | 0.897 | N=230<br>(low)            | N=22<br>(moderate)         |
| Inferior temporal gyrus,<br>posterior division     | 44.1 [40.5, 47.8]                | 45.2 [41.5, 48.9]                | 41.9 [37.7, 46.0]                | 9.2 [6.9, 11.6]     | 11.3 [9.0, 14.6]    | 0.926 | N=188<br>(low)            | N=18<br>(high)             |
| Inferior temporal gyrus,<br>temporo-occipital part | 43.3 [40.1, 46.5]                | 44.5 [40.9, 48.2]                | 41.7 [38.4, 45.1]                | 8.2 [6.5, 10.0]     | 10.7 [8.3, 12.8]    | 0.916 | N=152<br>(low)            | N=15<br>(high)             |
| Postcentral gyrus                                  | 64.0 [59.2, 68.9]                | 66.4 [61.4, 71.4]                | 64.4 [59.7, 69.1]                | 5.6 [4.3, 6.9]      | 7.6 [5.6, 9.2]      | 0.962 | N=71<br>(low)             | N=7<br>(high)              |
| Superior parietal lobule                           | 62.2 [57.1, 67.3]                | 64.1 [58.5, 69.7]                | 62.6 [57.0, 68.2]                | 5.6 [4.6, 6.6]      | 7.4 [5.9, 8.7]      | 0.973 | N=72<br>(low)             | N=7<br>(high)              |
| Supramarginal gyrus,<br>anterior division          | 55.4 [51.5, 59.4]                | 57.0 [53.0, 61.1]                | 55.9 [52.1, 59.7]                | 6.5 [5.1, 7.8]      | 8.8 [6.6, 10.3]     | 0.941 | N=90<br>(low)             | N=9<br>(high)              |
| Supramarginal gyrus,<br>posterior division         | 55.8 [51.9, 59.4]                | 56.4 [52.3, 60.6]                | 54.8 [51.0, 58.7]                | 5.9 [4.6, 7.1]      | 7.6 [6.0, 9.4]      | 0.953 | N=77<br>(low)             | N=8<br>(high)              |
| Angular gyrus                                      | 55.6 [51.8, 59.5]                | 57.0 [52.8, 61.2]                | 55.7 [51.9, 59.6]                | 5.8 [4.4, 7.2]      | 7.8 [5.8, 9.8]      | 0.947 | N=77<br>(low)             | N=8<br>(high)              |
| Lateral occipital cortex,<br>superior division     | 56.3 [52.0, 60.6]                | 58.5 [53.6, 63.4]                | 57.8 [52.9, 62.7]                | 5.7 [4.4, 7.0]      | 7.5 [5.6, 9.2]      | 0.962 | N=76<br>(low)             | N=8<br>(high)              |

**Table 5. Consistency of GM Blood Flow as Measured by pCASL (concluded)**

| Segment                                      | V1 Mean<br>[95% CI] <sup>a</sup> | V2 Mean<br>[95% CI] <sup>a</sup> | V3 Mean<br>[95% CI] <sup>b</sup> | MCV (%)<br>[95% CI] | MRD (%)<br>[95% CI] | ICC   | Rating<br>3% <sup>c</sup> | Rating<br>10% <sup>c</sup> |
|--|----------------------------------|----------------------------------|----------------------------------|---------------------|---------------------|-------|---------------------------|----------------------------|
| Lateral occipital cortex, inferior division  | 44.3 [40.6, 47.9]                | 45.8 [41.5, 50.1]                | 44.4 [40.5, 48.4]                | 7.8 [6.0, 9.5]      | 10.1 [7.8, 12.5]    | 0.930 | N=147<br>(low)            | N=14<br>(high)             |
| Intracalcarine cortex                        | 40.0 [36.6, 43.4]                | 41.5 [37.6, 45.4]                | 40.2 [36.1, 44.4]                | 8.1 [6.3, 10.0]     | 10.7 [8.1, 13.3]    | 0.927 | N=162<br>(low)            | N=15<br>(high)             |
| Frontal medial cortex                        | 50.4 [46.1, 54.7]                | 51.8 [48.2, 55.4]                | 48.3 [44.0, 52.5]                | 9.2 [7.2, 11.2]     | 12.0 [9.0, 15.0]    | 0.922 | N=193<br>(low)            | N=18<br>(high)             |
| Juxtapositional lobule cortex                | 69.5 [64.2, 74.8]                | 71.1 [66.3, 75.9]                | 67.7 [63.1, 72.3]                | 6.2 [4.9, 7.6]      | 8.1 [6.3, 10.1]     | 0.948 | N=90<br>(low)             | N=9<br>(high)              |
| Subcallosal cortex                           | 52.0 [47.8, 56.1]                | 53.1 [48.4, 57.7]                | 48.7 [44.1, 53.3]                | 11.6 [9.5, 13.4]    | 14.1 [12.1, 18.1]   | 0.896 | N=303<br>(low)            | N=28<br>(moderate)         |
| Paracingulate gyrus                          | 57.5 [53.1, 61.9]                | 58.4 [54.4, 62.5]                | 54.7 [50.1, 59.4]                | 7.4 [5.8, 9.1]      | 9.4 [7.3, 11.5]     | 0.940 | N=118<br>(low)            | N=12<br>(high)             |
| Cingulate gyrus, anterior division           | 56.0 [51.6, 60.4]                | 57.2 [53.6, 60.8]                | 54.5 [50.6, 58.4]                | 8.3 [6.6, 10.0]     | 10.8 [8.4, 13.2]    | 0.893 | N=155<br>(low)            | N=15<br>(high)             |
| Cingulate gyrus, posterior division          | 62.3 [58.2, 66.3]                | 63.7 [59.1, 68.3]                | 62.1 [57.4, 66.9]                | 5.7 [4.4, 7.1]      | 7.5 [5.6, 9.3]      | 0.947 | N=75<br>(low)             | N=8<br>(high)              |
| Precuneous cortex                            | 55.7 [51.6, 59.8]                | 58.2 [53.4, 62.9]                | 57.6 [52.7, 62.5]                | 5.9 [4.6, 7.2]      | 7.7 [6.0, 9.5]      | 0.959 | N=83<br>(low)             | N=8<br>(high)              |
| Cuneal cortex                                | 46.2 [42.4, 50.1]                | 47.7 [43.3, 52.0]                | 48.5 [43.6, 53.3]                | 7.0 [5.2, 8.8]      | 9.1 [6.6, 11.6]     | 0.946 | N=119<br>(low)            | N=12<br>(high)             |
| Frontal orbital cortex                       | 47.6 [44.2, 51.0]                | 49.4 [45.6, 53.1]                | 45.3 [41.3, 49.2]                | 8.0 [6.4, 9.7]      | 10.2 [8.1, 12.4]    | 0.947 | N=140<br>(low)            | N=14<br>(high)             |
| Parahippocampal gyrus, anterior division     | 37.4 [34.4, 40.4]                | 38.3 [35.0, 41.7]                | 35.9 [32.3, 39.5]                | 9.6 [7.2, 12.0]     | 12.2 [9.1, 15.2]    | 0.888 | N=206<br>(low)            | N=19<br>(high)             |
| Parahippocampal gyrus, posterior division    | 32.7 [30.6, 34.9]                | 33.8 [31.2, 36.4]                | 31.9 [29.4, 34.4]                | 6.9 [5.2, 8.7]      | 9.2 [6.7, 11.6]     | 0.900 | N=118<br>(low)            | N=12<br>(high)             |
| Lingual gyrus                                | 36.7 [33.8, 39.6]                | 38.2 [35.0, 41.5]                | 36.7 [33.4, 40.1]                | 8.2 [6.4, 10.0]     | 10.8 [8.3, 13.3]    | 0.920 | N=159<br>(low)            | N=15<br>(high)             |
| Temporal fusiform cortex, anterior division  | 33.9 [30.8, 37.0]                | 34.7 [31.7, 37.7]                | 31.4 [28.1, 34.7]                | 9.9 [6.9, 12.8]     | 12.3 [8.9, 15.7]    | 0.885 | N=237<br>(low)            | N=22<br>(moderate)         |
| Temporal fusiform cortex, posterior division | 33.2 [30.8, 35.5]                | 33.4 [31.0, 35.8]                | 31.5 [28.8, 34.2]                | 7.2 [5.5, 9.0]      | 9.1 [7.0, 11.3]     | 0.926 | N=116<br>(low)            | N=11<br>(high)             |
| Temporal occipital fusiform cortex           | 33.2 [30.7, 35.6]                | 33.4 [30.5, 36.3]                | 32.0 [29.0, 36.0]                | 8.5 [6.7, 10.3]     | 10.8 [8.5, 13.1]    | 0.909 | N=169<br>(low)            | N=16<br>(high)             |
| Occipital fusiform gyrus                     | 34.5 [31.7, 37.4]                | 36.2 [32.7, 39.7]                | 33.9 [30.5, 37.3]                | 8.0 [6.5, 9.6]      | 10.4 [8.3, 12.5]    | 0.937 | N=150<br>(low)            | N=14<br>(high)             |
| Frontal operculum cortex                     | 48.4 [44.8, 52.0]                | 49.4 [45.9, 52.9]                | 45.9 [41.9, 50.0]                | 7.9 [6.4, 9.4]      | 10.0 [8.2, 11.9]    | 0.934 | N=141<br>(low)            | N=14<br>(high)             |
| Central opercular cortex                     | 46.2 [43.0, 49.4]                | 47.7 [44.6, 50.8]                | 44.7 [41.6, 50.0]                | 7.4 [6.0, 8.9]      | 9.7 [7.7, 11.6]     | 0.907 | N=128<br>(low)            | N=12<br>(high)             |
| Parietal operculum cortex                    | 48.3 [45.1, 51.5]                | 48.5 [45.0, 52.0]                | 46.6 [43.2, 50.0]                | 7.8 [6.5, 9.1]      | 10.0 [8.4, 11.6]    | 0.907 | N=139<br>(low)            | N=13<br>(high)             |
| Planum polare                                | 48.2 [44.7, 51.7]                | 47.5 [44.0, 51.0]                | 43.7 [40.3, 47.1]                | 9.3 [8.0, 10.7]     | 11.8 [10.1, 13.5]   | 0.914 | N=197<br>(low)            | N=19<br>(high)             |
| Heschl's gyrus                               | 55.5 [50.8, 58.8]                | 54.9 [50.4, 59.4]                | 52.3 [48.0, 56.7]                | 7.9 [6.3, 9.4]      | 10.1 [8.1, 12.0]    | 0.930 | N=147<br>(low)            | N=14<br>(high)             |
| Planum temporale                             | 54.7 [50.5, 58.8]                | 54.1 [49.8, 58.4]                | 52.2 [48.1, 56.2]                | 7.5 [5.9, 9.1]      | 9.6 [7.5, 11.7]     | 0.925 | N=129<br>(low)            | N=13<br>(high)             |
| Supracalcarine cortex                        | 42.9 [39.3, 46.5]                | 43.9 [39.7, 48.1]                | 43.2 [38.8, 47.6]                | 8.5 [6.4, 10.5]     | 11.0 [8.1, 13.9]    | 0.917 | N=174<br>(low)            | N=17<br>(high)             |
| Occipital pole                               | 43.9 [40.2, 47.7]                | 44.8 [40.3, 49.4]                | 44.0 [39.6, 48.4]                | 9.8 [7.7, 12.0]     | 12.7 [9.8, 15.6]    | 0.900 | N=225<br>(low)            | N=21<br>(moderate)         |

<sup>a</sup>N=25.

<sup>b</sup>N=22 (three subjects completed only two visits).

<sup>c</sup>Reproducibility rating for 10% detection, power = 0.9, and significance = 0.05.

**Table 6. Consistency of WM Blood Flow as Measured by pCASL**

| Tract    | V1 Mean<br>[95% CI] <sup>a</sup> | V2 Mean<br>[95% CI] <sup>a</sup> | V3 Mean<br>[95% CI] <sup>b</sup> | MCV (%)<br>[95% CI] | MRD (%)<br>[95% CI] | ICC   | Rating<br>3% <sup>c</sup> | Rating<br>10% <sup>c</sup> |
|----------|----------------------------------|----------------------------------|----------------------------------|---------------------|---------------------|-------|---------------------------|----------------------------|
| Avg      | 7.39 [6.67, 8.12]                | 7.49 [6.70, 8.28]                | 7.32 [6.57, 8.08]                | 4.7 [3.2, 6.1]      | 6.3 [4.1, 8.1]      | 0.982 | N=49<br>(low)             | N=6<br>(high)              |
| Genu     | 11.7 [10.5, 12.8]                | 11.7 [10.5, 12.9]                | 11.3 [9.98, 12.6]                | 8.3 [6.3, 10.4]     | 10.7 [8.2, 13.1]    | 0.956 | N=136<br>(low)            | N=13<br>(high)             |
| Body     | 12.5 [11.3, 13.8]                | 13.0 [11.6, 14.4]                | 12.4 [10.9, 14.0]                | 8.6 [7.0, 10.2]     | 11.1 [9.1, 13.2]    | 0.961 | N=159<br>(low)            | N=15<br>(high)             |
| Splenium | 9.84 [8.83, 10.9]                | 9.90 [8.71, 11.1]                | 9.37 [8.07, 10.7]                | 9.8 [7.3, 12.3]     | 12.1 [9.3, 15.0]    | 0.950 | N=200<br>(low)            | N=19<br>(high)             |
| FX       | 6.95 [5.84, 8.07]                | 7.49 [6.51, 8.47]                | 6.80 [5.91, 7.69]                | 19.3 [14.1, 24.6]   | 27.1 [18.5, 35.8]   | 0.872 | N=757<br>(low)            | N=69<br>(low)              |
| CS       | 3.38 [2.31, 4.46]                | 3.74 [2.61, 4.87]                | 3.19 [2.11, 4.27]                | 47.4 [33.3, 61.5]   | 76.3 [40.1, 112.6]  | 0.900 | N=2690<br>(low)           | N=243<br>(low)             |
| IC       | 10.9 [9.63, 12.1]                | 11.3 [9.99, 12.7]                | 10.5 [9.12, 12.0]                | 11.4 [9.2, 13.6]    | 15.3 [12.1, 18.6]   | 0.946 | N=263<br>(low)            | N=25<br>(moderate)         |
| CR       | 9.33 [8.23, 10.4]                | 9.71 [8.53, 10.9]                | 9.05 [7.87, 10.2]                | 9.8 [7.8, 11.8]     | 12.7 [10.1, 15.4]   | 0.947 | N=219<br>(low)            | N=21<br>(moderate)         |
| Tr       | 9.16 [8.04, 10.3]                | 9.49 [8.28, 10.7]                | 8.91 [7.68, 10.1]                | 10.6 [7.8, 13.3]    | 13.5 [9.7, 17.3]    | 0.949 | N=241<br>(low)            | N=23<br>(moderate)         |
| SS       | 9.34 [8.28, 10.4]                | 9.94 [8.73, 11.2]                | 8.77 [7.73, 9.81]                | 10.2 [7.4, 12.9]    | 13.1 [9.7, 17.4]    | 0.949 | N=229<br>(low)            | N=22<br>(moderate)         |
| EC       | 11.9 [10.8, 13.0]                | 12.5 [11.3, 13.7]                | 11.4 [10.2, 12.7]                | 10.4 [7.9, 13.0]    | 13.4 [10.1, 16.7]   | 0.926 | N=223<br>(low)            | N=21<br>(moderate)         |
| Cing     | 17.1 [15.3, 19.0]                | 17.4 [15.6, 19.3]                | 16.5 [14.2, 18.7]                | 10.0 [7.2, 12.7]    | 13.3 [9.3, 17.4]    | 0.953 | N=203<br>(low)            | N=19<br>(high)             |
| SLF      | 11.2 [9.93, 12.5]                | 11.7 [10.3, 13.2]                | 11.0 [9.49, 12.5]                | 10.9 [8.1, 13.7]    | 14.4 [10.2, 18.6]   | 0.935 | N=249<br>(low)            | N=25<br>(moderate)         |
| FO       | 10.2 [8.82, 11.5]                | 10.7 [9.30, 12.0]                | 10.1 [8.78, 11.5]                | 13.3 [10.5, 16.1]   | 17.9 [13.1, 22.6]   | 0.919 | N=382<br>(low)            | N=35<br>(moderate)         |

<sup>a</sup>N=25.

<sup>b</sup>N=22 (three subjects only completed two visits); mean values for three visits in units of mL/100 g/min.

<sup>c</sup>Reproducibility rating for 10% detection, power = 0.9, and significance = 0.05.

For WM TE135 spectroscopy, MCV and MRD were the lowest in tNAA (reflecting N-acetylaspartate and N-acetylaspartylglutamate) compared to total choline (Cho) (reflecting glycerophosphocholine and phosphocholine) and tCr (reflecting Cr and phosphocreatine) (Table 7; ICC range 0.851–0.962). WM TE30 for frontal lobe trended lower in consistency (Table 7; ICC range 0.565–0.886), with tCho being the most consistent and tCr least consistent in terms of ICC. Again, tNAA had the lowest MCV and MRD and GSH had the highest MCV and MRD values. GM TE30 for AC metabolites (Table 7; ICC range 0.667–0.879) was similar, with tCho most consistent and tCr least consistent in terms of ICCs, while tNAA had the lowest MCV and MRD values and GSH had the highest values. All measurements were high on the 3% and 10% reproducibility rating scale except for the TE30 frontal lobe (Glu, mI, Glu+Gln and TE30 AC (Glu+Gln)).

Utilization of repeated MRI measurements for longitudinal studies of disease progression and treatment effects depends on the reproducibility of MRI measurements. The inherent technical and physiological variability in MRI measurements may contribute to measurement errors and interfere with detection of change due to advancing pathological or therapeutic changes. Multiple technical factors contribute to variability on repeat imaging, including variability in MRI scanners, sequences, MRI technicians, and MRI interpretation. No structural change over a short interval in a healthy cohort would be anticipated. Physiological variability, however, including activity level change, diurnal variation, or nutritional and/or alcohol intake, might impact measurements. Prior to interpreting the effect of a disease state, reproducibility or consistency must be known. The aim of this study of 25 healthy subjects is to provide reference

data on intrasubject variability by controlling for these other factors, thus establishing a baseline power level to help with understanding the statistical significance of the observed changes.

**Table 7. Consistency of Proton MRS**

| Metabolite                    | V1 Mean<br>[95% CI] <sup>a</sup> | V2 Mean<br>[95% CI] <sup>a</sup> | V3 Mean<br>[95% CI] <sup>b</sup> | MCV (%)<br>[95% CI] | MRD (%)<br>[95% CI] | ICC   | Rating<br>3% <sup>c</sup> | Rating<br>10% <sup>c</sup> |
|-------------------------------|----------------------------------|----------------------------------|----------------------------------|---------------------|---------------------|-------|---------------------------|----------------------------|
| <i>TE135 Frontal Lobes WM</i> |                                  |                                  |                                  |                     |                     |       |                           |                            |
| Mean tCho                     | 1.91 [1.81, 2.01]                | 1.86 [1.78, 1.94]                | 1.89 [1.79, 1.99]                | 3.9 [3.1, 4.7]      | 5.0 [3.9, 6.0]      | 0.962 | N=35<br>(moderate)        | N=4<br>(high)              |
| Mean tNAA                     | 11.0 [10.6, 11.4]                | 11.0 [10.7, 11.4]                | 10.9 [10.6, 11.3]                | 2.8 [1.8, 3.9]      | 3.7 [2.3, 5.1]      | 0.914 | N=19<br>(high)            | N=3<br>(high)              |
| Mean tCr                      | 5.05 [4.89, 5.21]                | 5.0 [4.80, 5.12]                 | 5.03 [4.87, 5.19]                | 4.1 [3.1, 5.1]      | 5.3 [4.0, 6.7]      | 0.851 | N=38<br>(moderate)        | N=5<br>(high)              |
| <i>TE30 Frontal Lobes WM</i>  |                                  |                                  |                                  |                     |                     |       |                           |                            |
| Frontal mean<br>Glu           | 8.16 [7.73, 8.60]                | 7.74 [7.41, 8.08]                | 7.91 [7.45, 8.36]                | 7.8 [6.3, 9.3]      | 10.1 [7.9, 12.2]    | 0.816 | N=141<br>(low)            | N=14<br>(high)             |
| Frontal mean<br>tCho          | 2.27 [2.14, 2.41]                | 2.23 [2.13, 2.32]                | 2.27 [2.12, 2.42]                | 6.4 [4.6, 8.2]      | 8.3 [5.8, 10.7]     | 0.886 | N=91<br>(low)             | N=9<br>(high)              |
| Frontal mean<br>tNAA          | 9.98 [9.62, 10.3]                | 9.92 [9.61, 10.23]               | 9.86 [9.51, 10.2]                | 4.7 [2.9, 6.6]      | 6.1 [3.7, 8.4]      | 0.694 | N=51<br>(low)             | N=6<br>(high)              |
| Frontal mean<br>mI            | 5.51 [5.24, 5.78]                | 5.34 [5.02, 5.66]                | 5.31 [4.99, 5.63]                | 8.2 [6.2, 10.2]     | 10.7 [8.1, 13.3]    | 0.745 | N=155<br>(low)            | N=15<br>(high)             |
| Frontal mean<br>tCr           | 7.32 [7.06, 7.57]                | 7.01 [6.81, 7.22]                | 7.02 [6.75, 7.30]                | 6.1 [4.3, 7.9]      | 7.7 [5.3, 10.1]     | 0.565 | N=84<br>(low)             | N=9<br>(high)              |
| Frontal mean<br>Glu+Gln       | 9.86 [9.30, 10.4]                | 9.59 [9.22, 9.95]                | 9.62 [9.10, 10.1]                | 7.2 [5.7, 8.6]      | 9.0 [7.0, 11.1]     | 0.818 | N=119<br>(low)            | N=12<br>(high)             |
| FRONTAL mean<br>GSH           | 2.44 [2.28, 2.59]                | 2.36 [2.24, 2.49]                | 2.31 [2.10, 2.51]                | 11.3 [8.2, 14.5]    | 14.1 [10.6, 17.6]   | 0.696 | N=281<br>(low)            | N=26<br>(moderate)         |
| <i>TE30 AC WM</i>             |                                  |                                  |                                  |                     |                     |       |                           |                            |
| AC Glu                        | 13.3 [12.8, 13.7]                | 13.4 [13.1, 13.7]                | 13.0 [12.6, 13.4]                | 4.2 [3.3, 5.1]      | 5.5 [4.2, 6.7]      | 0.763 | N=43<br>(low)             | N=5<br>(high)              |
| AC GSH                        | 2.43 [2.32, 2.55]                | 2.46 [2.35, 2.58]                | 2.42 [2.33, 2.52]                | 6.1 [4.6, 7.6]      | 7.8 [5.9, 9.8]      | 0.798 | N=87<br>(low)             | N=9<br>(high)              |
| AC tCho                       | 2.20 [2.08, 2.31]                | 2.23 [2.14, 2.31]                | 2.18 [2.07, 2.28]                | 4.8 [3.5, 6.2]      | 6.3 [4.4, 8.2]      | 0.879 | N=52<br>(low)             | N=6<br>(high)              |
| AC tNAA                       | 11.4 [11.1, 11.6]                | 11.4 [11.2, 11.6]                | 11.4 [11.2, 11.6]                | 2.5 [1.8, 3.2]      | 3.2 [2.3, 4.1]      | 0.787 | N=15<br>(high)            | N=3<br>(high)              |
| AC mI                         | 6.65 [6.38, 6.91]                | 6.75 [6.53, 6.98]                | 6.62 [6.40, 6.85]                | 4.3 [3.2, 5.4]      | 5.6 [4.2, 6.9]      | 0.781 | N=44<br>(low)             | N=6<br>(high)              |
| AC tCr                        | 10.4 [10.2, 10.7]                | 10.4 [10.2, 10.6]                | 10.2 [10.0, 10.4]                | 2.9 [2.2, 3.6]      | 3.8 [2.8, 4.7]      | 0.667 | N=21<br>(moderate)        | N=3<br>(high)              |
| AC Glu+Gln                    | 15.1 [14.6, 15.6]                | 15.2 [14.8, 15.5]                | 15.0 [14.5, 15.5]                | 4.6 [3.6, 5.5]      | 5.9 [4.6, 7.2]      | 0.765 | N=51<br>(low)             | N=4<br>(high)              |

<sup>a</sup>N=25.

<sup>b</sup>N=22 (three subjects only completed two visits); mean metabolites are in institutional units.

<sup>c</sup>Reproducibility rating for 10% detection, power = 0.9, and significance = 0.05.

Our approach of three scanning sessions and tightly controlled methodological parameters provides for the opportunity to assess these measurements based on the normal physiological variance among them. WMH quantification for subcortical lesion volume/count was highly reproducible. Similarly, periependymal WMH volume was reproducible, but count less so. Pulsation of ventricular CSF and subject motion may cause artifacts, with partial volume averaging impeding accurate segmentation of small (<1 cm<sup>3</sup>) periependymal lesions. Subcortical lesions are unaffected by CSF pulsation artifacts and had higher ICC. We believe that higher variance in periependymal count measurements is secondary to these artifacts, making accurate identification of small periependymal lesions more challenging. This effect is further exaggerated by much smaller (3–5 times) number and volume of lesions in this healthy sample, compared to those reported in the general population, magnifying the effect of misidentifying even a single small lesion.

Overall whole-brain average and regional cortical GM thickness and volumetric measurements showed excellent ICC and other measures of reproducibility that were consistent with other published results. The cortical GM thickness of the entorhinal, insula, and medial orbitofrontal demonstrated lower reproducibility. These three cortical GM areas are located on the inferior frontal portion of the brain where susceptibility artifacts due to tissue-bone interface make the precise identification of boundaries more difficult. Therefore, caution is recommended when interpreting cortical GM thickness findings from these areas.

Whole-brain FA was highly reproducible, with individual tracts showing only slightly reduced reproducibility metrics than the whole-brain average FA. The least consistency was observed in FX, CS, and superior FO tracts. The lack of consistency on these three tracts can be explained by partial volume averaging and/or spatial misregistration. The FX and CS are long, tubular WM that pass through the areas with magnetic susceptibility and therefore are prone to geometrical distortions. Measurements of the unrestricted water fraction  $M_u$  and PDI from the diffusion-weighted data collected in the WM of CC were highly reproducible. The same measurements performed in the AC GM were more variable, suggesting tissue-specific variance in normal physiology. There are two potential sources of variability in the AC. The variance in diffusion-based measurements is likely to be influenced by normal day-to-day physiological variability in the GM. The higher variance may also be due to methodological sources, as the measurements from the dense and consistently oriented fibers of the CC may have greater reproducibility than the measurements from the cortical GM ribbon that is adjacent for WM and CSF. The tissue-related difference in the reproducibility was likewise observed in the resting CBF as measured by pCASL. The whole-brain average CBF in cerebral WM showed higher reproducibility than in cerebral GM, while the AC gyrus was lower. Our results are consistent with other reported studies. Our results suggest pCASL can be utilized for comparison studies of whole-brain and segment GM CBF. Additionally, while whole-brain and CC WM CBF is highly reproducible, other WM tracts have greater variability.

MRS assessment of neurochemical concentrations using a standard, clinical, long TE (TE = 135 ms) protocol demonstrated high reproducibility in frontal WM for tCho, tNAA, and tCr.

### **5.3 Multimodal WM Responses to Hypoxic Hypobarica in Humans**

No significant change was demonstrated between Aircrew Fundamentals Course subjects and controls in structural measurements such as FLAIR assessment of WMHs or FA for baseline MRI and subsequent MRI data. Significant differences were observed between MRI#1 and MRI#2 in WM CBF (white matter – WM-ASL) but not in GM CBF (gray matter – GM-ASL) (Table 8). ASL showed an upregulation of WM and GM CBF at both 24 and 72 hours in the exposed subjects (WM  $p = 0.003/0.020$ ; GM  $p = 0.053/0.041$ ). Group comparison using a generalized additive model adjusted for age and gender demonstrated significant increased WM CBF at 24 and 72 hours post-exposure compared to controls ( $p < 0.001$  and  $p = 0.048$ , respectively). There is no statistical difference in CBF between the 24- and 72-hour MRIs. No significant change in CBF was observed in the control subjects.

**Table 8. Arterial Spin Labeling Changes in White and Gray Matter**

| MRI           | Aircrew Fundamentals Course<br>Mean±SE<br>(mL/100 g/min) | Controls<br>Mean±SE<br>(mL/100 g/min) |
|---------------|--|---------------------------------------|
| <b>WM-ASL</b> |  |                                       |
| MRI#1         | 7.045±0.171  | 7.003±0.199                           |
| MRI#2         | 7.311±0.161  | 6.909±0.194                           |
| MRI#3         | 7.255±0.162  | 7.083±0.193                           |
| <b>GM-ASL</b> |  |                                       |
| MRI#1         | 50.160±0.762   | 50.798±1.054                          |
| MRI#2         | 50.691±0.753   | 50.713±1.032                          |
| MRI#3         | 50.918±0.785   | 50.570±1.054                          |

SE = standard error.

## 6.0 DISCUSSION

Repetitive occupational exposure to nonhypoxic hypobaric exposure has been associated with clinical symptoms and MRI changes consistent with focal and diffuse axonal injury in cerebral WM. The symptoms and MRI findings are similar to those observed in mild traumatic brain injury and are consistent with a form of diffuse axonal injury. We demonstrated highly reproducible MRI data for neuroimaging measurements, making them valuable for evaluation of disease states and treatment protocols.

We observed no significant changes in WM integrity, as assessed by FA, following a 20-minute exposure to hypobaria accompanied by 2-5 minutes of hypoxia. We observed a significant upregulation of WM CBF 24 hours after exposure to hypobaria and hypoxia that did not return to baseline 72 hours post-exposure. The mechanisms of hypo- and hyperbaric damage to the cerebral WM are unknown, but activation of innate immune response triggered by occlusion of microcapillaries by microbubbles and particles is possible. Hypo- and hyperbaric exposure in aviators and divers, respectively, has been associated with presence of both venous and arterial microbubbles and, in divers, production of blood-borne microparticles. We observed large individual differences in the WM CBF response that was unrelated to structural differences among subjects. Instead, the state of cerebral neuroprotective stores was predictive of the degree of upregulation in the WM CBF. MRS measurements were used to provide baseline levels of the neurometabolites supporting the basal levels of cellular energy stores, metabolism and antioxidant capacity (NAA, Glu+Gln, GSH), and the indicators of the ongoing inflammatory activity (mI and Cho). Subjects with lower baseline levels of the neurometabolites that support normal cell functions showed progressively higher CBF response in cerebral WM. We observed no significant changes in structural indices of WM integrity at 24 and 72 hours post-exposure. Likewise, we observed no effect of the baseline structural WM integrity on the changes in WM CBF following exposure. This is arguably because of the uniform excellent health state of the subjects. For instance, all the subjects in this sample had only very minor WMH burden, which is consistent with their age and the state of health. Overall, this supports the safety of the hypobaric exposure protocol as used by the USAF and the North Atlantic Treaty Organization with a clinical incidence of DCS of 0.26%.

## 7.0 CONCLUSIONS

We demonstrated highly reproducible MRI data for neuroimaging measurements, making them valuable for evaluation of disease states and treatment protocols. We demonstrated compelling evidence of transient brain injury from a single exposure to hypobaria as evidenced by increase CBF, persisting at 72 hours post-exposure, and transient neurometabolite changes (GSH, Cho, Glu, NAA, ml, Cr). The duration of elevated CBF after a single altitude chamber hypobaric exposure is not yet known. Changes in CBF may be driven by neurometabolite changes. A higher WMH baseline burden seems to predict greater CBF change (significant in WM-ASL data). This suggests a potential underlying susceptibility to injury and possible synergy between hypobaric exposure and hypoxia. WMHs in pilots/aircrew are likely a function of both frequency and cumulative effects of decompressive stress from hypobaric exposure.

## 8.0 REFERENCES

1. Jersey SL, Hundemer GL, Stuart RP, West KN, Michaelson RS, Pilmanis AA. Neurological altitude decompression sickness among U-2 pilots: 2002-2009. *Aviat Space Environ Med.* 2011; 82(7):673-682.
2. McGuire SA, Sherman PM, Brown AC, Robinson AY, Tate DF, et al. Hyperintense white matter lesions in 50 high-altitude pilots with neurologic decompression sickness. *Aviat Space Environ Med.* 2012; 83(12):1117-1122.
3. McGuire SA, Sherman PM, Profenna L, Grogan P, Sladky J, et al. White matter hyperintensities on MRI in high-altitude U-2 pilots. *Neurology.* 2013; 81(8):729-735.
4. McGuire SA, Sherman PM, Wijtenburg SA, Rowland LM, Grogan PM, et al. White matter hyperintensities and hypobaric exposure. *Ann Neurol.* 2014; 76(5):719-726.
5. McGuire SA, Tate DF, Wood J, Sladky JH, McDonald K, et al. Lower neurocognitive function in U-2 pilots: relationship to white matter hyperintensities. *Neurology.* 2014; 83(7):638-645.
6. Wardlaw JM, Smith C, Dichgans M. Mechanisms of sporadic cerebral small vessel disease: insights from neuroimaging. *Lancet Neurol.* 2013; 12(5):483-497.
7. U.S. Air Force. Aerospace physiological training program. Washington (DC): Department of the Air Force; 2012. Air Force Instruction 11-403. [Accessed 1 Apr 2018]. Available from [http://static.e-publishing.af.mil/production/1/af\\_a3/publication/afi11-403/afi11-403.pdf](http://static.e-publishing.af.mil/production/1/af_a3/publication/afi11-403/afi11-403.pdf).
8. Alsop DC, Detre JA, Golay X, Günther M, Hendrikse J, et al. Recommended implementation of arterial spin-labeled perfusion MRI for clinical applications: a consensus of the ISMRM perfusion study group and the European consortium for ASL in dementia. *Magn Reson Med.* 2015; 73(1):102-116.
9. Gasparovic C, Neeb H, Feis DL, Damaraju E, Chen H, et al. Quantitative spectroscopic imaging with in situ measurements of tissue water T1, T2, and density. *Magn Reson Med.* 2009; 62(3):583-590.

## LIST OF ABBREVIATIONS AND ACRONYMS

|               |   |
|---------------|---|
| <b>AC</b>     | anterior cingulate                                    |
| <b>ASL</b>    | arterial spin labeling                                |
| <b>CAL</b>    | calibration study subjects                            |
| <b>CBF</b>    | cerebral blood flow                                   |
| <b>CC</b>     | corpus callosum                                       |
| <b>Cho</b>    | choline   |
| <b>CI</b>     | confidence interval                                   |
| <b>Cing</b>   | cingulum  |
| <b>Cr</b>     | creatine  |
| <b>CR</b>     | corona radiata  |
| <b>CS</b>     | corticospinal tract                                   |
| <b>CSF</b>    | cerebrospinal fluid                                   |
| <b>CTRL</b>   | control subject                                       |
| <b>DCS</b>    | decompression sickness                                |
| <b>DTI</b>    | diffusion tensor imaging                              |
| <b>EC</b>     | external capsule                                      |
| <b>ENIGMA</b> | enhanced neuro imaging genetics through meta-analysis |
| <b>FA</b>     | fractional anisotropy                                 |
| <b>FLAIR</b>  | fluid-attenuated inversion recovery                   |
| <b>FO</b>     | fronto-occipital                                      |
| <b>FOV</b>    | field of view   |
| <b>FX</b>     | fornix  |
| <b>GLM</b>    | generalized linear model                              |
| <b>Gln</b>    | glutamine   |
| <b>Glu</b>    | glutamate   |
| <b>GM</b>     | gray matter   |
| <b>GSH</b>    | glutathione   |
| <b>HARDI</b>  | high angular resolution diffusion imaging             |
| <b>IC</b>     | internal capsule                                      |
| <b>ICC</b>    | intraclass correlation                                |

|                      |  |
|----------------------|--|
| <b>KS</b>            | Kolmogorov-Smirnov                       |
| <b>MBI</b>           | multi- <i>b</i> -value diffusion imaging |
| <b>MCV</b>           | mean coefficient of variation            |
| <b>mI</b>            | myo-inositol                             |
| <b>MRD</b>           | mean relative difference                 |
| <b>MRI</b>           | magnetic resonance imaging               |
| <b>MRS</b>           | magnetic resonance spectroscopy          |
| <b>M<sub>u</sub></b> | unrestricted water component             |
| <b>NAA</b>           | N-acetylaspartate                        |
| <b>NEX</b>           | number of excitations                    |
| <b>pCASL</b>         | pseudocontinuous arterial spin labeling  |
| <b>PDI</b>           | permeability-diffusivity index           |
| <b>ROBD</b>          | reduced oxygen breathing device          |
| <b>SE</b>            | standard error                           |
| <b>SLF</b>           | superior longitudinal fasciculus         |
| <b>SNR</b>           | signal-to-noise ratio                    |
| <b>SS</b>            | sagittal stratum                         |
| <b>TE</b>            | time of echo                             |
| <b>Tr</b>            | thalamic radiation                       |
| <b>TR</b>            | time of repetition                       |
| <b>USAF</b>          | U.S. Air Force                           |
| <b>WHASC</b>         | Wilford Hall Ambulatory Surgical Center  |
| <b>WM</b>            | white matter                             |
| <b>WMH</b>           | white matter hyperintensity              |